Hung, Sing-Chang

CALCULATIONS OF CHEMISORPTION OF HYDROGEN AND NITROGEN ON TITANIUM USING X-ALPHA-SW AND SCF-CI METHODS

City University of New York PH.D. 1983

PLEASE NOTE:

In all cases this material has been filmed in the best possible way from the available copy. Problems encountered with this document have been identified here with a check mark ✓.

1. Glossy photographs or pages _____
2. Colored illustrations, paper or print _____
3. Photographs with dark background ✓
4. Illustrations are poor copy _____
5. Pages with black marks, not original copy _____
6. Print shows through as there is text on both sides of page _____
7. Indistinct, broken or small print on several pages ✓
8. Print exceeds margin requirements _____
9. Tightly bound copy with print lost in spine _____
10. Computer printout pages with indistinct print _____
11. Page(s) _____ lacking when material received, and not available from school or author.
12. Page(s) _____ seem to be missing in numbering only as text follows.
13. Two pages numbered _____. Text follows.
14. Curling and wrinkled pages _____
15. Other _____

CALCULATIONS OF CHEMISORPTION OF HYDROGEN AND NITROGEN ON TITANIUM USING $X\alpha$-SW AND SCF-CI METHODS

by

SING-CHANG HUNG

A dissertation submitted to the Graduate Faculty in Physics in partial fulfillment of the requirements for the degree of Doctor of Philosophy, The City University of New York.

1982

This manuscript has been read and accepted for the Graduate Faculty in Physics in satisfaction of the dissertation requirement for the degree of Doctor of Philosophy.

Oct. 20, 1982
date

C. R. Fisher
Chairman of Examining Committee

Oct. 26, 1982
date

Joel Kirsten
Executive Officer

Fred J. Cadieu

Raymond T. Disch

Luke A. Burke

Frank Martins
Supervisory Committee

The City University of New York

Abstract

CALCULATIONS OF CHEMISORPTION OF HYDROGEN AND NITROGEN ON TITANIUM USING Xα-SW AND SCF-CI METHODS

by

SING-CHANG HUNG

Adviser: Professor C. Rutherford Fischer

Two theoretical studies are used as examples of chemisorption on transition metal surfaces. The first calculation employs the SCF-Xα-SW method to determine the electronic structures of several close-packed Ti-Ti and Ti-H systems. The relative importance of Ti s, p, and d electron bonding to its Ti neighbors and to H are reported. The roles of the d electrons in the Ti-Ti and Ti-H bond are discussed. The effect of the presence of an H atom on the first few layers of the metal is also studied. The second set of calculations employs the Hartree-Fock-Roothaan SCF formulation supplemented by configuration-interaction (CI) to determine the energetics of adsorption of an N_2 molecule at a Ti surface. These calculations are made tractable by using a Ti core potential and by a unitary localization transformation to define a local surface region of localized lattice plus adsorbate orbitals. The results show that an underlayer of N atoms forms at the octahedral sites. The calculated

adsorption energy of 115 kcal/mole compares favorably with experiment. Binding energy contributions in the several successive steps of the calculations are discussed. Eigenvalue spectra for the selected lattice-adsorbate geometries are compared to the UPS experimental data.

DEDICATION

I dedicate this effort, and
the good that it represents,
to my wife and my parents with

love

ACKNOWLEDGEMENTS

I express my gratitude to Professor C. Rutherford Fischer for providing me with the opportunity and guidance to complete this work. His encouragement, knowledge and patience were invaluable to me.

Furthermore, I thank the entire faculty and staff of the Physics Department of Queens College of The City University of New York for their friendship and support. In particular, I am grateful to Professor Fred Cadieu for his useful discussions, Mr. Walter Koch for drawing many of the Figures, Miss Anne Jeng for typing this manuscript, and to the two lovely secretaries, Mrs. Shirley Allen and Mrs. Susan Wasserman for their assistance.

TABLE OF CONTENTS

LIST OF TABLES

LIST OF ILLUSTRATIONS

CHAPTER I

INTRODUCTION

I-1 Introduction

If a solid surface is exposed to a vapor, molecules of the vapor may adhere to the solid surface. If this adhesion involves some kind of strong electronic interaction with a heat of adsorption greater than 15 kcal/mole[1], the process is referred to as CHEMISORPTION. However if no such interaction occurs, the process is called physical, or van der Waals' adsorption.

A chemisorption bond does not differ in principle from ordinary chemical bonds, and is due to the same electrostatic forces which operate in atoms and molecules. The only special feature of the chemisorptive bond is that it can, depending on the circumstances, be composed of many highly delocalized molecular orbitals, a situation which is seldom encountered in ordinary chemical bonds.

I-2 Background

The interaction of atoms and molecules with metal surfaces is an important problem both from a practical viewpoint and because a basic understanding of chemisorption and catalysis is lacking at the molecular level.[2,3,4] Among the topics for which a molecular description is needed are coverage of the surface by the adsorbate, adsorption and desorption processes, existence of active sites and their deactivation, and composition and geometry of the surface. Recently, experimental techniques for studying surface configurations and dynamics of reactions on surfaces of known geometry have advanced rapidly.[5] Photoelectron Spectroscopy and low energy electron diffraction (LEED) results are readily compared to theory. Thus there is a need for corresponding advances in the theoretical development.

Since Lennard-Jones[6] proposed a theory of chemisorption in 1932, many calculations of adsorbate-surface interactions have been carried out. However, no quantitative theory fulfilling basic requirements for an understanding of catalysis and chemisorption is presently available. Such a theory would yield dissociation energies and activation barrier values as well as geometries which are accurate enough to distinguish active sites. This theory should also be able to adequately describe both ground and low lying excited electronic states in order to make possible the description of scattering and reactions at the surface.

One type of theoretical approach to the description of the electronic structures of surfaces uses calculational solid state

techniques which describe infinite and semi-infinite solids. These include Jellium,[7] LCAO,[8] Green's function,[9] and pseudopotential theories.[10] Some of these methods have been used for descriptions of adsorbate-surface interactions.[11] The local density exchange approximation[12,13] has recently offered a means to merge the solid state and molecular (described below) viewpoints to some extent. Several applications of this type of technique, two versions of which are the self consistent field Xα scattered wave[12] and Hohenberg-Kohn-Sham methods,[13] have been made to adsorbate solid interactions.[14] We employ the Xα-SW method to study Ti-H systems.

Molecular theory at the SCF-CI level may also be applied to adsorbate-metal lattice chemisorption and it is this approach which we also decided to use here. The method as formulated by Whitten and co-workers[15] involves a unitary transformation to localize some lattice orbitals at the active site. These orbitals are then treated together with the adsorbate orbitals at the configuration-interaction (CI) level. This treatment, which includes effects significantly beyond the Hartree-Fock approach (correlation energy) is expected to be able to accurately describe the formation and breaking of bonds which occur during adsorption. Here the method will be applied to determine a few important points on the potential energy surface describing the interaction between N_2 and a titanium lattice surface.

I-3 Self-Consistent-Field $X\alpha$ Scattered-Wave Cluster Method (SCF-$X\alpha$-SW)

The SCF-$X\alpha$-SW method[16] was originally developed to study the electronic structures of solids.[17,18] Recently this method has been applied extensively to polyatomic molecular problems and also to chemisorption. The SCF-$X\alpha$-SW method, when solved using the so-called muffin tin approximation, divides the cluster space into three regions: sphere (atomic) region, intersphere (interatomic) region and outersphere (exterior) region. The division is shown in Figure I-1. The one-electron Schrödinger equation is set up for a so-called "muffin-tin" approximation to the true potential. A spherically symmetrical potential obtained by averaging over angles is used within the spheres surrounding the various nuclei and for the outersphere region, while volume averaging is used to obtain the constant valued intersphere potential. The one-electron Schrödinger equation is solved separately for each region, but observing the boundary conditions for the regions. This is a multiple-scattering method, equivalent to the Korringa-Kohn-Rostoker (KKR) method[17,18] often used for infinite lattices. Once the eigenfunctions and eigenvalues of this problem are determined, one assumes that the orbitals of lowest eigenvalue are occupied, up to the Fermi level. From the resulting charge densities, one can compute a total energy, using a statistical approximation for the exchange correlation. This approximation has an undetermined factor α (whence the name $X\alpha$ method). It is frequently neccessary to re-populate the levels between succesive iterations. This ensures that,

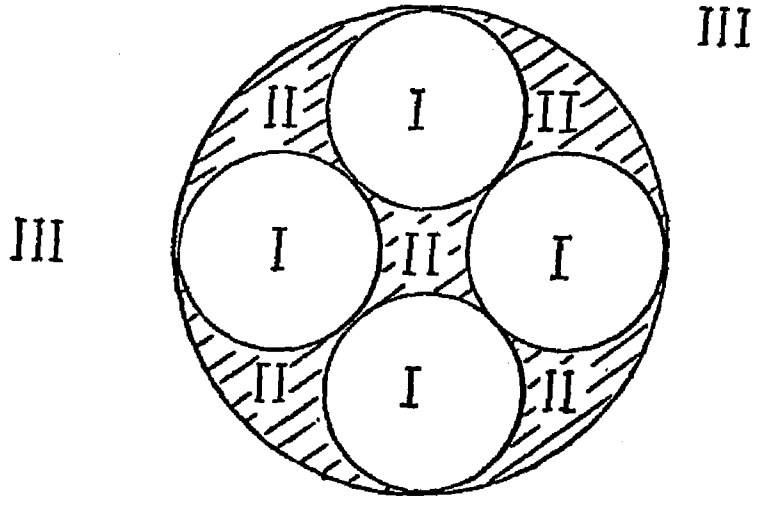

I-Sphere region (atomic region)

II-Intersphere region (interatomic region)

III-Outersphere region (exterior region)

Figure I-1 Three regions of the cluster space

in the ground-state configuration, all spin orbitals with energies below the Fermi level are fully occupied, allowing for partial occupancy only at the Fermi energy itself, and is consistent with the fact that the Xα theory rigorously satisfies Fermi statistics.[19,20] The value of α for an isolated atom is determined by requiring that the total energy, using the statistical approximation, should equal the precise Hartree-Fock energy.

The Xα-SW method is a self-consistent field numerical method when solved in the muffin-tin approximation. Following Connolly and Johnson,[21] the mathematical formulation is described as follows: The Xα potential has the form (in Hartree atomic units)

$$V(\vec{r}) = -\sum_j \frac{Z_j}{|\vec{r} - \vec{R}_j|} + \sum_i \int \frac{\psi_i^*(\vec{r}')\psi_i(\vec{r}')}{|\vec{r} - \vec{r}'|} d\vec{r}' - 3\alpha\left[\frac{3}{8\pi}\sum_i \psi_i^*(\vec{r})\psi_i(\vec{r})\right]^{1/3}, \qquad \text{.....(I-1)}$$

where Z_j is nuclear charge for the atom at position R_j. The functions ψ_i are the solutions to the set of equations which somewhat resemble the Hartree-Fock equations:

$$[\nabla_i^2 + V_\alpha(\vec{r})]\psi_i(\vec{r}) = \varepsilon_i\psi_i(\vec{r}) \qquad \text{.....(I-2)}$$

where ε_i are the one-electron eigenvalues and α is an "exchange scaling parameter". The averaged potential is defined according to the following equations:

$$V(\vec{r}) = \bar{V}_p(\vec{r}_p) = \frac{1}{4\pi} \iint V_\alpha(\vec{r})\sin\theta_p \, d\theta_p \, d\phi_p, \qquad 0 \le r_p \le b_p;$$

$$= \bar{V}_0(\vec{r}_0) = \frac{1}{4\pi} \iint V_\alpha(\vec{r}) \sin\theta_0 \, d\theta_0 \, d\phi_0, \qquad b_0 \leq r_0 < \infty ;$$

$$= \bar{V}_{in} = \frac{1}{\Omega_{in}} \iiint_{\Omega_{in}} V_\alpha(\vec{r}) d\vec{r}, \qquad \text{otherwise,}$$

.....(I-3)

where $\vec{r}_p = \vec{r} - \vec{R}_p$ and $\vec{r}_0 = \vec{r} - \vec{R}_0$. In eqs. (I-3), and the following equations, we have labelled those quantities referring to the outer-sphere region by subscript 0, and the atoms in the molecule by p=1,2,...N. In this expression, b_p is the radius of the pth atomic sphere, R_p is the position vector of the sphere center, b_0 is the radius of the outer sphere which defined the outersphere region, and Ω_{in} is the volume of the interatomic region (intersphere region)

$$\Omega_{in} = \frac{4}{3}\pi \left(b_0^3 - \sum_{p=1}^{N} b_p^3\right) \qquad \text{.....(I-4)}$$

The solutions of eq. (I-2) for the averaged potential (I-3) can now be expressed. In the atomic region, for the rth atom, ψ_i will be a linear combination of spherical functions

$$\psi_i = \sum_{lm} C_{lm}^{ip} \; u_l^p(r_p, \varepsilon_i) \; Y_{lm}(\hat{r}_p), \qquad \text{.....(I-5)}$$

where the C_{lm}^{ip} are linear coefficients to be determined, the Y_{lm} are real spherical harmonics and u_l^p is a radial function which satisfies the differential equation

$$\frac{1}{2r^2}\ \frac{d}{dr}\ (r^2\frac{du_l}{dr}) + (\ \frac{l(l+1)}{r^2} + \bar{V}_p(r) - \varepsilon_i)\ u_l = 0 \qquad \cdots\cdots(I\text{-}6)$$

where the one electron energy ε_i is left as a variable to be determined in the final equations. In the outersphere region, the wave functions will have a similar expansion with undetermined coefficients. In the interatomic region, since the potential there is a constant, we can expand the wave function as a linear combination of free-space functions:

$$\psi_i = \sum_{lm}\{\ A_{lm}^{i0} j_l(kr_0)\ Y_{lm}(\hat{r}_0) + \sum_{p=1}^{N} A_{lm}^{ip} f_l(kr_p)\ Y_{lm}(\hat{r}_p)\} \qquad \cdots\cdots(I\text{-}7)$$

where

$$k = (\varepsilon_i - \bar{V}_{in})^{\frac{1}{2}}, \qquad \cdots\cdots\cdots\cdots\cdots\cdots\cdots\cdots(I\text{-}8)$$

$$f_l(kr) = h_l^{(1)}(kr) \qquad \varepsilon_i < \bar{V}_{in} \text{ (k imaginary);}$$

$$= n_l(kr) \qquad \varepsilon_i > \bar{V}_{in} \text{ (k real).} \qquad \cdots\cdots(I\text{-}9)$$

In the above expressions, j_l is a spherical Bessel function, n_l is a spherical Neumann function and $h_l^{(1)}$ is a spherical Hankel function of the first kind while the A_{lm}^{ip} are linear coefficients to be determined.

The C- and A- coefficients, and the energies ε_i are determined by demanding that ψ_i and its first derivative be continuous at each

sphere boundary. This condition leads directly to a set of linear equations for the A-coefficients

$$[t_l^p(\varepsilon_i)]^{-1} A_{lm}^{ip} = \sum_{q\neq p} \sum_{l'm'} G_{lm;l'm'}^{pq}(\varepsilon_i) A_{l'm'}^{iq} , \qquad \cdots\cdots\cdots(I\text{-}10)$$

in which

$$t_l^p(\varepsilon) = \{W[j_l(kr), u_l^p(r)]/W[f_l(kr), u_l^p(r)]\}_{r=b_p} ,$$
$$\cdots\cdots\cdots(I\text{-}11)$$
$$t_l^0(\varepsilon) = \{W[f_l(kr), u_l^0(r)]/W[j_l(kr), u_l^0(r)]\}_{r=b_0} ,$$

and the G-coefficients, referred to as "structure factors", are defined by the equations:

$$G_{lm;l'm'}^{pq} = -4\pi i^{l-l'} \sum_{LM} i^{-L} I_{LM}(lm;l'm') f_L(kR_{pq}) Y_{LM}(\hat{R}_{pq}), \quad q\neq 0,$$
$$\cdots\cdots\cdots(I\text{-}12)$$
$$G_{lm;l'm'}^{po} = -4\pi i^{l-l'} \sum_{LM} i^{-L} I_{LM}(lm;l'm') j_l(kR_{po}) Y_{LM}(\hat{R}_{po}),$$

$W(u,v)=u(dv/dr) - v(du/dr)$ is a Wronskian function and

$$I_{LM}(lm;l'm') = \int\int Y_{lm}(\hat{r}) Y_{LM}(\hat{r}) Y_{l'm'}(\hat{r}) \sin\theta \, d\theta \, d\phi \qquad \cdots\cdots\cdots(I\text{-}13)$$

are Gaunt coefficients. $\vec{R}_{pq} = |\vec{R}_p - \vec{R}_q|$ are the interatomic distances. If one of the atoms is centered at $\vec{R}_0$, then $R_{po} = 0$ and $G_{lm;l'm'}^{po}(E)=\delta_{ll'}\delta_{mm'}$.

The C-coefficients are also determined by the boundary conditions and are related to the A-coefficients by the relations

$$A^{ip}_{lm} = -ikb_p^2\{W[j_l(kr),\ u^p_l(r,\varepsilon_i)]\}_{r=b_p}\ C^{ip}_{lm}\ ,$$

$$A^{io}_{lm} = -ikb_p^2\{W[u^o_l(r,\varepsilon_i),\ f_l(kr)]\}_{r=b_o}\ C^{io}_{lm}\ . \qquad \text{.....(I-14)}$$

The one-electron energies ε_i are then found as the zeroes of the determinant of the coefficients in the set of linear equations (I-10):

$$\det\{[t^p_l(\varepsilon_i)]^{-1}\delta_{ll'}\delta_{mm'}\delta_{pq} - G^{pq}_{lm;l'm'}(\varepsilon_i)\} = 0. \qquad \text{.....(I-15)}$$

The secular equation can be block-diagonalized into smaller determinants by the use of the symmetry properties of the cluster. For the first iteration in the self-consistent procedure, we set the charge density equal to a superposition of the densities derived from Xα calculations for the isolated atoms. A potential is then generated by means of eq. (I-1). An averaged potential is then calculated according to the definitions of eq. (I-3). By numerical integrations (eq. (I-6)) the functions $u^p_l(\vec{r},\varepsilon_i)$ are generated and substituted into the secular equation (I-15). Since the determinant is a non-linear function of ε_i, eq. (I-15) cannot be solved directly. It must be evaluated for several values of ε_i and solved by inverse interpolation. The eigenfunctions corresponding to each ε_i are then found through eq. (I-10) and (I-14). The charge density derived from these eigenfunctions

is then used to generate a potential for the next iteration. This process is continued until self-consistency is achieved.

The "SCF-Xα-SW" model has been successfully applied to a wide range of polyatomic molecules and to clusters simulating local environments in nonmetalic solids.[22] This method has also been proved to be suited for the study of small transition- and noble-metal clusters.[23] The method has the following characteristics:

(1) It leads to an accurate solution of a model Hartree-Fock problem without undue computational effort.

(2) It should be of particular advantage in treating large polyatomic systems.

(3) It has the rapid convergence characteristic of partial-wave methods.

(4) It is an ab initio technique, but has the flexibility of semiempirical methods through the incorporation of a few adjustable parameters.

(5) It is not necessary to treat the core- and valence- electron or σ- and π- electron problems differently, or to neglect their interaction. Both are handled self-consistently as parts of the same calculation.

(6) It can be used as an ideal first step toward a calculation which employs a less restricted form of potential and toward a calculation which deals with the total wavefunction and its energy. In the latter application, the method of configuration interaction can be adapted, in principle, to the present scheme in order to take into account the effects of correlation.

I-4 SCF-CI Method

The SCF-CI method we use was designed particularly for the chemisorption study of metallic surfaces.[15,24] We use this method to study the chemisorption of molecules on transition metal surfaces using a nitrogen molecule on a titanium lattice surface as our example. Starting with the usual Hartree-Fock-Roothaan SCF formulation[25] for the lattice plus adsorbate, a local surface region is defined and a unitary localization transformation is carried out on the lattice orbitals. The configuration interaction (CI) calculations using these localized orbitals plus adsorbate orbitals provide an accurate description of the lattice- adsorbate interaction. Figure I-2 shows a schematic outline of the SCF-CI method. The detailed description of the SCF-CI method is described as follows:

A. Treatment of the metal atom lattice and atomic cores.

The SCF-CI method starts with the restricted Hartree-Fock theory to describe the transition-metal cluster. Atomic core electrons are assumed to be localized, but give rise to Coulomb and exchange potentials which are accurately evaluated along with contributions due to core-valence orbital overlap. Core-valence overlap consideration are usually handled by constructing a pseudopotential for the valence electrons. In our present method, the valence basis functions of a given atom are rigorously orthogonalized to the core orbitals of that atom using a simple auxiliary basis. The Gram-Schmidt orthogonalization method is applied to introduce the core orbitals into the valence space. This method

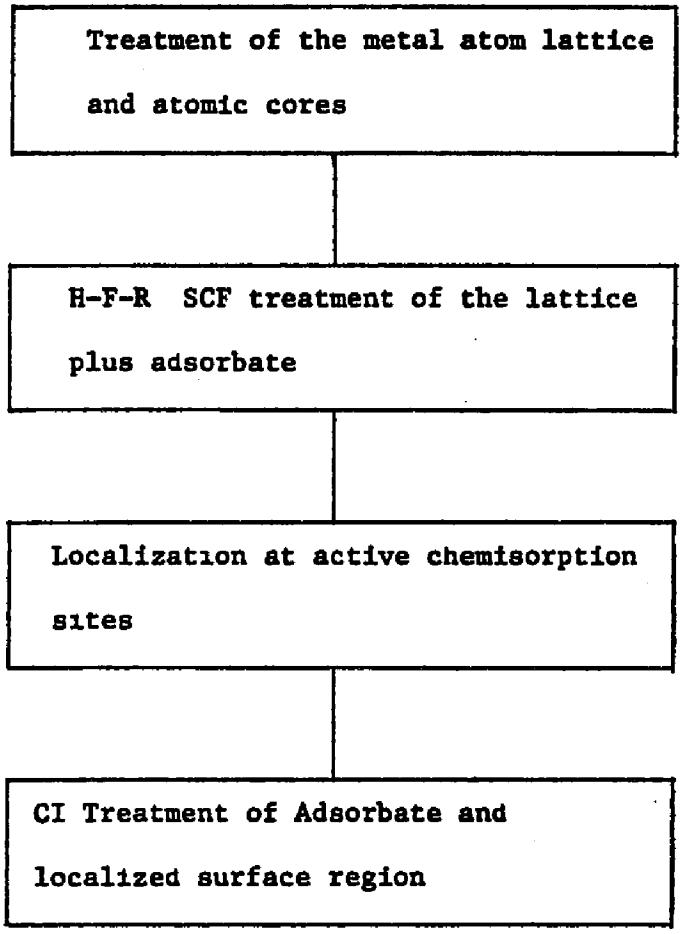

Figure I-2 Scheme Outline of the SCF-CI Method.

of core-valence overlap consideration is described in detail in Whitten and Pakkanen's paper.[15]

B. Hartree-Fock-Roothaan SCF treatment of the lattice plus adsorbate

For the adsorbate, the atomic cores are not assumed to be localized. Therefore, all electrons which belong to the adsorbate are treated as valence electrons and are involved in the entire SCF calculation. Now we include the lattice and adsorbate in a single SCF calculation. The result of the SCF calculation on the whole system (lattice atoms plus adsorbate) is a single determinant total wave function for the N valence electrons of the system

$$\psi = R(\phi_1, \phi_2, \ldots \phi_N) \qquad \text{(I-16)}$$

(R is an antisymmetric function)

where the ϕ_k are orthonormal spin orbitals. For instance, for titanium the ground configuration is $1s^2 2s^2 2p^6 3s^2 3p^6 3d^2 4s^2$ and the valence basis for expansion of ϕ_k could be chosen as $4s_j$ plus additional function $4s_j'$ on nucleus j. An extra $3d_j$ function is added to the expansion of ϕ_k for the titanium atoms near the active chemisorption sites. For the nitrogen molecule the ground configuration is $1s^2 2s^2 2p^3$ and the valence basis for expansion of ϕ_k could be chosen as $1s_k$, $2s_k$, $2p_{xk}$, $2p_{yk}$, $2p_{zk}$ plus $1s'_k$, $2s'_k$, $2p'_{xk}$, $2p'_{yk}$ and $2p'_{zk}$ on nucleus k. Occupancies of incompletely filled d shells must be chosen carefully to avoid unfavorable repulsion resulting from a double occupancy of spatial d orbitals. That also means that Hund's rule should be obeyed on every atomic center. Roothaan's SCF theory for open shells of electronic systems[26] can be employed for this purpose.

C. Localization at active chemisorption sites

In metallic systems the valence orbitals are delocalized so that a strictly local description is not possible. But by an orbital localization procedure it is expected that the essential features of the adsorbate-surface interaction are obtained by treating the chemisorption site accurately. An approximate field of the lattice is included in the description by inclusion of the initial delocalized orbitals in the calculation, as a fixed CI core.

The localization is carried out as follows. The SCF orbitals of the whole lattice-adsorbate system $\{\phi_k\}$ are obtained in the usual single-determinant wave-function form. Then a second set of atomic orbitals $\{\chi_k\}$ of the designated chemisorption site is chosen. Then the set $\{\phi_k\}$ is transformed by applying a unitary transformation to obtain a new set $\{\phi_k'\}$ subject to maximization of the sum of exchange integrals Γ

$$\Gamma = \sum_{k=1}^{M} [\chi_k(1)\phi'(1)| \frac{1}{r_{12}} |\chi_k(2)\phi'(2)] \geq 0 \qquad \cdots\cdots\cdots\cdots (I\text{-}17)$$

where $\phi' = \sum_i C_i\phi_i$ is a transformed orbital. This leads to an eigenvalue problem with solutions, ordered in eigenvalues

$$\Gamma_1 \geq \Gamma_2 \geq \cdots\cdots \geq \Gamma_N,$$

$$\Gamma_1 : \phi_1' = \sum_i C_{i1}\phi_i,$$

Footnote: The M of Eq. (I-17) represents the total number of valence orbitals of the designated chemisorption site.

$\Gamma_2 : \phi_2'$

. . .

$\Gamma_p : \phi_p'$

.....(I-18)

$\Gamma_{p+1} : \phi_{p+1}'$

. . .

$\Gamma_N : \phi_N' = \sum_i C_{iN} \phi_i$

The resulting total wave function

$$\psi = R(\phi_1'\phi_2'.....\phi_N') \qquad .....(I-19)$$

is identical to the initial wave function $\psi = R(\phi_1\phi_2.....\phi_N)$. Now we find that after some member Γ_p in the eigenvalue spectrum, the orbitals $\phi_{p+1}'.....\phi_N'$ exhibit negligible exchange interaction with the representative orbitals, $\{\chi_k\}$. The functions $\phi_1'\phi_2'....\phi_p'$ physically represent orbitals localized on the designated atoms, bonds between these atoms, and bonds linking the designated atoms with the remainder of the lattice.

Similarly, it is also of interest to carry out a localizing transformation within the virtual space since the resulting localized orbitals are those orbitals primarily needed for configuration interaction refinement of the local region.

This localization scheme leads to the existence of a dual orbital space, one associated with the active chemisorption site, and one

associated with the rest of the lattice. The dual nature of the resultant orbital space is in contrast to other localization schemes.[27,28,29] For instance, the Ruedenberg exchange maximization method[27] does not have this dual nature.

The objective of this localization scheme is to define an interior part of the lattice electron distribution which can be taken as invariant during the course of interaction with the chemisorption site, and to introduce the important (delocalization) characteristics of an extended lattice into the concept of a local region near the surface. The same purpose can apply to the adsorbate as well.

D. CI Treatment of Adsorbate and Localized Surface Region

The final stage of the calculation is to carry out a configuration interaction (CI) calculation at the chemisorption site. CI is necessary for an accurate description of bonding for many reasons. For example, the unpaired d electrons in Ti can couple in many different ways and leads to a multitude of states near the ground state.[30,31] The relative occupation of d and s orbitals is a major question in chemisorption and affects the binding characteristics at the site. CI is ideally suited to the study of participation of various states. Configuration mixing also yields accurate dissociation energy curves since variable ionic and covalent character of the binding is allowed.

Following Whitten and Pakkanen,[15] the CI wave function is

$$\psi = \sum_k C_k \psi_k \qquad \text{.....(I-20)}$$

with $\psi_k = A(\Phi_1,\ldots\Phi_M, \Phi'_{M+1},\ldots\Phi_N')$

Here, A is the usual anti-symmetrizing operactor. There are M electrons in the chemisorption region and N-M further "invariant core" orbitals mainly associated with the lattice. The "invariant core" contributes a fixed field experienced by the M electron orbitals. The calculation proceeds with the successive diagonalization procedure of Whitten and Hackmeyer[32,33] and involves diagonalization of the secular determinant in several successive steps.

CHAPTER II

SOME EXPERIMENTAL METHODS USED IN CHEMISORPTION STUDIES

II-1 Low Energy Electron Diffraction (LEED)

II-1-1 Introduction

In 1924 deBroglie suggested[34] that particles such as atoms, electrons and neutrons might show dual character, exhibiting the properties of waves as well as those of particles. He proposed that the wavelength λ, associated with those particles be given by

$$\lambda = \frac{h}{mv} = \frac{h}{(2mE)^{\frac{1}{2}}} \qquad \text{.....(II-1)}$$

where m and v and E are, respectively, the mass, velocity, and kinetic energy of the particle and h is Planck's constant. For electrons this relation becomes

$$[E(eV)]^{\frac{1}{2}} = \frac{12}{\lambda(\text{A}^{\circ})} \qquad \text{.....(II-2)}$$

The diffraction of electrons that were back scattered from the surface of a nickel crystal was observed by Davisson and Germer in 1927.[35] Only a few studies were performed during the thirty year period since 1928. Most of the accomplishments of LEED research have been carried out in the late 60's and early 70's. Since then the LEED experiment has become the major technique to determine the surface structure of metals.[36,37] The first successful structure analysis by LEED experiment of an underlayer of nitrogen atoms on a clean

titanium metal surface was reported by Shih and co-workers in 1976.[38]

Electrons are scattered by the atomic potential. Low energy (5-200eV) electrons, owing to their charge, are predominantly scattered by the surface atoms. Therefore, Low-Energy Electron Diffraction plays the same role in the study of surfaces as X-ray diffraction plays in the study of the bulk structure.[39] Since the atomic surface density ($\sim 10^{15}/cm^2$) is much smaller than the bulk density of atoms ($\sim 10^{22}/cm^3$), once the incident beam has penetrated over approximately 10 atomic planes, the X-ray diffracted beam contains no easily detectable information about the surface atoms. However LEED uses the diffracted beam from the surface atoms and provides us with important information about the structure of crystal surfaces.

II-1-2 Diffraction Conditions

In a LEED experiment a mono-energetic beam of electrons is incident on a crystal surface. The incident electron beam can be described by a plane wave $\psi(\vec{r})$ in free space at a given point $\vec{r}$:

$$\psi(\vec{r}) = \psi(0)\, e^{i[\vec{k}\cdot\vec{r} - \omega t]} \qquad \text{.....(II-3)}$$

Here $\psi(0)$ is the wavefunction at an arbitrary origin, $\vec{r} = 0$ amd $\vec{k}$ is the wave vector of the traveling wave which has an angular frequency ω. For simplicity, we can assume $\psi(0) = 1$. For a given $\vec{k}$, i.e. for incident electron of well-defined wavelength $\lambda = \frac{2\pi}{|\vec{k}|}$ it can be

readily shown[40] that the electrons are scattered by a periodic three-dimensional lattice only in well-defined directions corresponding to wave vectors satisfying the condition

$$\vec{k}' = \vec{k} + \vec{G} \qquad \text{.....(II-4)}$$

where $\vec{k}'$ is the wave vector of the scattered beam and $\vec{G}$ is the reciprocal lattice vector. Diffraction can occur only if the magnitude of the incident and scattered wave vectors remain the same, $|\vec{k}'| = |\vec{k}|$. That is, the diffraction process is elastic. A typical diffraction condition is shown in Figure II-1.

Since $|\vec{G}(hkl)| = \dfrac{2\pi n}{d(hkl)}$ (h, k, l are the Miller indices) (n is an integer)

and $|\vec{G}(hkl)| = |\Delta\vec{k}| = 2|\vec{k}|\sin\theta$

then $$\frac{2\pi n}{d(hkl)} = 2|\vec{k}|\sin\theta \qquad \text{.....(II-5)}$$

where d is the spacing between planes (h,k,l) of the crystal and θ is the half-angle between the scattering vectors $\vec{k}$ and $\vec{k}'$.

Since $|\vec{k}| = \dfrac{2\pi}{\lambda}$, we have arrived at the Bragg reflection law:

$$n\lambda = 2d \sin\theta \qquad \text{.....(II-6)}$$

For LEED the wave vector $\vec{k}$ in units of Å^{-1} is uniquely defined by the electron beam energy as

$$|\vec{k}| = \frac{2\pi}{\lambda} = 0.512\sqrt{E(eV)} \qquad \text{.....(II-7)}$$

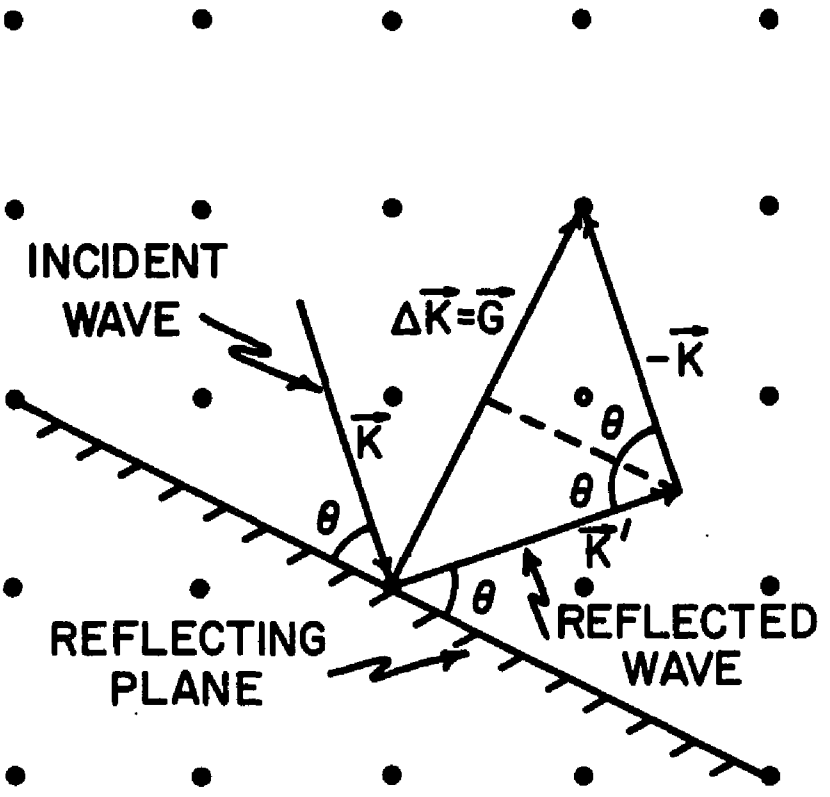

Figure II-1 Determination of $\Delta\vec{k} = \vec{k}'-\vec{k}$ in terms of angle of scattering θ.

II-1-3 Apparatus for LEED Experiment

In a typical LEED apparatus low-energy electrons are produced by heating a metal or an oxide filament (cathode) in vacuum. The emitted electrons are drawn off toward the anode by a suitable accelerating potential. Although most of the electrons will strike the anode walls, a small fraction of them escapes through a hole in the anode structure. These electrons are then focused magnetically or electrostatically (approximate beam size $1mm^2$) and are allowed to impinge on the surface of a single crystal.

Figure II-2 shows schematically the apparatus most frequently used in LEED studies. The crystal in most experiments is maintained at ground potential with respect to the negative cathode. After allowing the scattered electrons to drift radially away from the crystal surface, the separation of the elastic and inelastic components is made by using a retarding potential (applied to a grid) that repels all inelastically scattered electrons, thus allowing only the elastically scattered electrons to penetrate. The elastically scattered electrons, after passage through the retarding field, are post accelerated by a positive potential and impinge on a spherical fluorescent screen where the diffraction pattern is displayed.

II-1-4 Data Analysis of LEED Experiment and Possible LEED Information for Chemisorption

Diffraction patterns and intensities of the diffraction spots are the two most important types of data we can get from a LEED

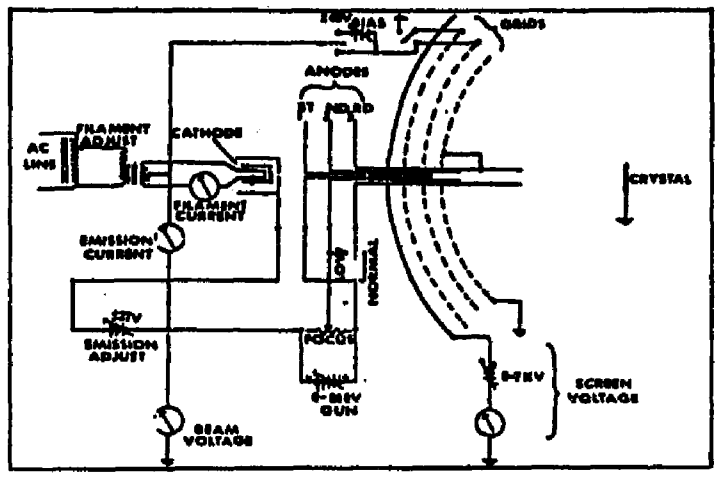

Figure 1-2 *Scheme of the low-energy electron diffraction apparatus employing the postacceleration technique.*

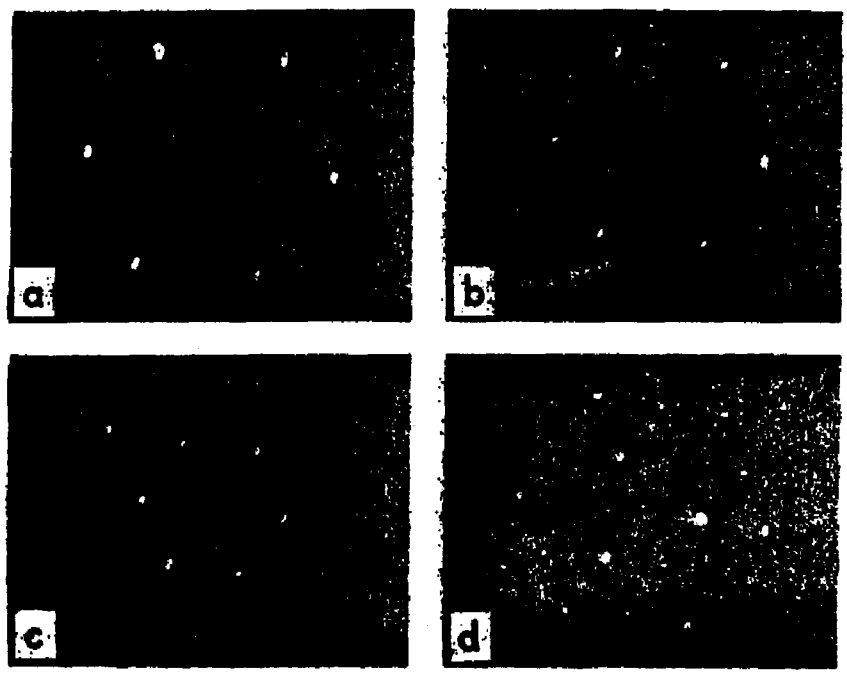

Figure 1-3 *Diffraction pattern of the (111) face of platinum single crystal at four different incident electron beam energies: (a) 51 volts; (b) 63.5 volts; (c) 160 volts; (d) 181 volts.*

Figures taken from : G. A. Somorjai, Principles of Surface Chemistry, p.31 & p.33 Prentice-Hall, Inc.(1972)

experiment. A typical set of diffraction patterns for scattering from a clean (111) face of a platinum single crystal is shown in Figure II-3 for various electron energies. The relative distances of the diffraction spots and their symmetry in a diffraction pattern can be used to determine the size of the surface unit cell that characterizes the arrangement of surface atoms. The intensity of a diffraction spot depends on the dynamic scattering factors (atomic scattering factor and structrue factor of the basis). From the diffraction pattern's complement of the intensities of the diffraction spots we are able to determine the unique position of atoms in the unit cell.

In the study of chemisorption phenomenon, we are interested in the following questions:

(a) What is the atomic configuration of an adsorbed particle with respect to the surface atoms of the chemisorbed layer?

(b) What configurations do the adsorbed particles have relative to each other?

Question (a) is related to the theory of the chemisorption bond,[41] whereas, (b) is related to the interactions between the adsorbed particles and can be treated theoretically by statistical methods.[42] With the helpful information of the diffraction patterns and the intensities of the diffraction spots, we can easily see that question (b) may be answered immediately in those cases where the primitive cell contains only one adsorbed particle. This condition is frequently fulfilled. However, an answer to question (a) from

LEED-information can be achieved in only a few special cases where additional arguments are available. In general, utilization of the information from LEED patterns may be limited to a unique characterization of the adsorbed state only.

In many systems the arrangement of the adsorbed particles is not perfectly periodic. If the periodic regions are relatively small the diffraction spots are broadened. From the spot diameter the size of the ordered domain can be estimated and the symmetry of the adsorption sites can also be derived.

II-2 ULTRAVIOLET PHOTOEMISSION SPECTROSCOPY (U.P.S.)

II-2-1 Introduction

When a photon beam with an energy between 6 and 100 ev or high-energy electromagnetic radiation (x-ray with an energy about 50 kev) is allowed to strike the solid surface, in addition to electron emission from the valence band, electrons are excited from inner electron shells as well.[43] The two primary inner-shell excitation processes are illustrated in Figure II-4. The notation we have adopted is that most commonly used in atomic spectroscopy: the K. L, M,...shells refer to the shells with principal quantum number n=1,2,3,...and the subscripts (L_I,L_{II},L_{III}) indicate the multiplicity $\vec{j}$, which is the vector sum of the angular momentum $\vec{l}$ and the spin quantum number $\vec{s}$; $\vec{j}=\vec{l}+\vec{s}$.

When an atom absorbs a photon an electron may be ejected from any inner shell into vacuum. This process is called photoelectron emission. If the energy of the incident photon or radiation is greater than the binding energy of the electron, photoelectron emission can take place. From the knowledge of the incident beam energy and suitable analysis of the ejected photoelectrons, the electronic binding energies for the different bands can be obtained. Energy analysis of the emitted photoelectrons is called photoelectron spectroscopy. Ultraviolet photoemission spectroscopy uses an incident photon beam with energy within the ultraviolet energy region (5 ev < E_{photon} < 200 ev).

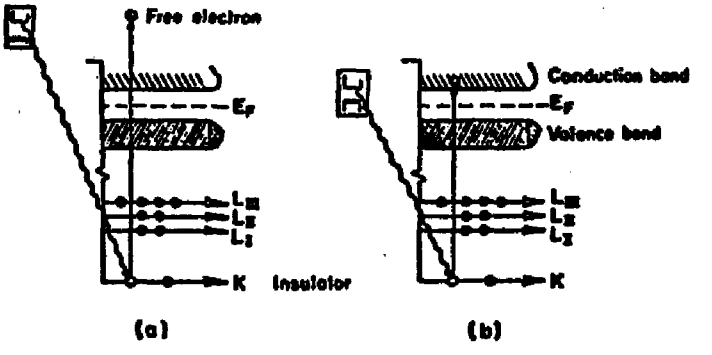

Figure II-4 Energy-level-diagram representation of (a) photoelectron emission and (b) x-ray absorption.

Figure taken from : G. A. Somorjai, Principles of Surface Chemistry, p.175, Prentice-Hall, Inc.(1972)

The study of chemisorption is only interesting for the surface bonding states with bonding energy less than 10 ev below the Fermi energy. Therefore the low energy ultraviolet photoemission spectroscopy (6 ev < $E_{photon} \leq 100$ ev) is suitable to this study.

II-2-2 Apparatus for UPS Experiments

The apparatus commonly used is shown schematically in Figure II-5. A monochromatic ultraviolet photon beam is incident on the sample, which is prepared in an ultra-high-vacuum chamber, and is the source of the ejected photoelectrons. The emitted electrons are detected by the detector and energy-analyzed by the energy analyzer together with associated electronics for recording energy distributions. The available ultraviolet photon sources are the Hinteregger-type lamp (E_{photon} < 11.6 ev) and the cold-cathode resonance lamp, with radiation at 21.2 and 40.8 ev provided by He (I) and He (II) and radiation at 16.8 ev and 26.9 ev provided by Ne (I) and Ne (II) lines.[44] The energy of the ejected photoelectron, E_{obs}, depends on the incident photon energy $h\nu_{photon}$ and is given by

$$E_{obs} = h\nu_{photon} - E_b - \phi_a \quad \text{.....(II-8)}$$

Here E_b is the electron binding energy in the shell from which it is ejected and ϕ_a is the work function of the analyzer. The electronic binding energy is thus directly calculable from Eg (II-8).

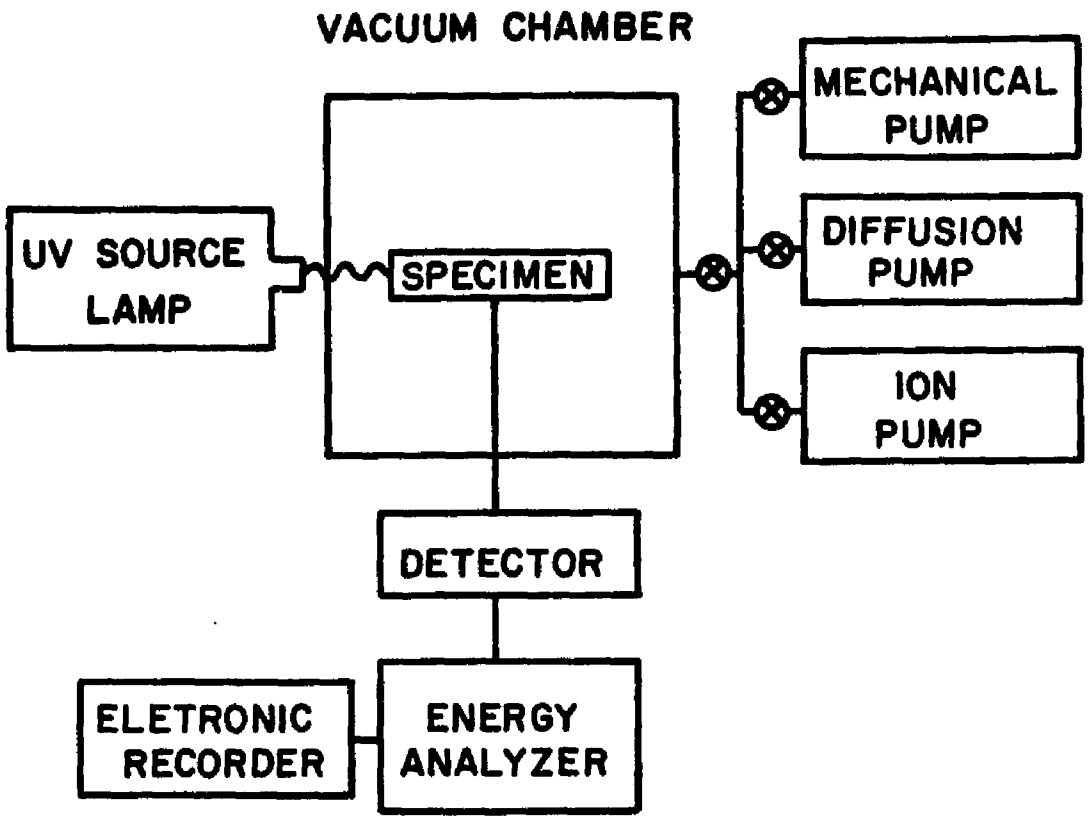

Figure II-5 Apparatus for UV Photoelectron Spectroscopy.

II-2-3 Data Analysis of UPS Experiment and Possible UPS Information for Chemisorption Studies

In Figure II-6 a typical photoelectron spectrum is shown. The experimental density of states derived from the photoemission energy spectrum is expected to bear a close resemblance to the electronic density of states.[45] The intensity of the peaks can be used to determine the relative or absolute concentration of different elements. In addition to the detection of elemental chemical composition, ultraviolet photoelectron spectroscopy can distinguish between the different oxidation states of an element due to the shift in the binding energies of inner shell electrons upon change of valency.[46] This is called the chemical shift.

By monitoring chemical shifts, UPS has not only been able to distinguish between different oxidation states but also to detect other changes in the chemical environment that lead eventually to the determination of the electron density. That means that chemical shifts can be used to distinguish between surface and bulk atoms and to monitor the changing chemical environment of surface species.

The study of chemisorption processes is also concerned with asking the following in addition to Questions (a) and (b) in section II-1-4.

(c) What is the binding energy of each state in the chemisorbed system?

(d) What is the chemical shift of the new chemisorbed system relative to the old bulk system?

(e) What is the density of states of the new chemisorbed system?

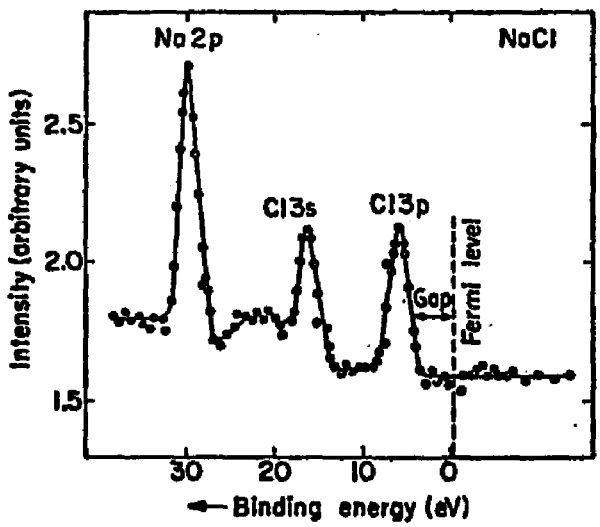

Figure *II-6 Photoelectron spectrum of sodium chloride.*

Figure taken from : G. A. Somorjai, Principles of Surface Chemistry, p.182, Prentice-Hall, Inc.(1972)

The data of LEED experiments are not capable of answering these questions. Fortunately, UPS can compensate for this weakness of LEED and provide the answers to these three additional questions.

CHAPTER III

ELECTRONIC STRUCTURE OF TITANIUM CLUSTERS USING THE Xα-SW METHOD

III-1 Background

Transition-metal-atom interactions have been the subject of a number of recent molecular-orbital calculations. The bonding between metal atoms and the interaction of metals with hydrogen have been studied in connection with models for chemisorption on metal surfaces. Melius et al.[31] and Melius[47] have studied the dissociation of H_2 on reaction with Ni_2 using multiconfigurational self-consistent field (SCF) methods and have discussed the role of s, p, and d electrons in chemisorption. According to their analyses the d electrons remain localized and do not participate directly in bonding; however the d orbitals can serve as a source or reservoir for the valence σ electrons as the state or geometry varies. This type of model for the d electrons seems to be consistent with generalized valence-bond and unrestricted Hartree-Fock calculation carried out by Kunz and co-workers on ScH and MnH.[48] Configuration-interaction calculations on TiH also indicate a limited role for the d electrons in the Ti-H bond.[49,50] Recent ab initio SCF calculations on linear chains of Ti atoms have also been reported to show a high degree of d localization.[50]

In contrast to the localized d model, however, other recent calculations have shown considerable d-electron transfer or sharing in metal-metal and metal-absorbate bonding. These pictures arise

naturally from band-structure, molecular-orbital, and hybrid-orbital reasoning.[51] In particular, Xα-SW calculations by Messmer et al.[52] of H-atom interactions with Ni, Pd and Pt clusters indicate a strong role for the d orbitals in the bonding of the H atom to the surface of the transition-metal cluster. They conclude that clusters of more than two metal atoms are needed to study properly the role of d orbitals in chemisorption, and that the second transition-metal series can exhibit different d-orbital behavior from the first series. The importance of d-orbital bonding is also emphasized in another Xα-SW calculation by Rosch and Rhodin[53] for bonding with a cluster of Ni atoms.

In 1979, Fischer and Whitten[30] studied the interactions between Ti and a H atom and between Ti atoms in chains of length two, five and ten by using the Xα-SW method. Their calculation confirmed a significant d participation in bonding. However, their calculation also raises some uncertainties mainly due to the rapid increase in intersphere volume compared to intrasphere volume as the chain length increases (cubic versus linear). The role of the effect of the constant potential on the d orbitals needs a more detailed investigation.

As the cluster size increases, it is expected that the electronic structure of a cluster will come to resemble that of the bulk material if the method being used is valid. For the bulk titanium, there is some evidence that the configuration is $(3d)^3\ (4s)^1$ compared with $(3d)^2\ (4s)^2$ for the titanium atom.[54] The configuration of $(3d)^3\ (4s)^1$

for bulk titanium has been applied in the ab initio SCF calculation[15] even though the ab initio SCF calculation only uses a cluster to represent a bulk. The size of a Ti cluster which will behave more or less like a bulk Ti is not known yet. A study of this question is necessary. Bulk titanium is a non-magnetic material while the titanium atom has a net spin of one. To see how this happens requires a systematic study with several different sizes of titanium clusters.

Titanium was chosen in the present study to minimize uncertainties in the theoretical treatment of transition metals. Intrashell correlation for the d electrons is expected to be less important in Ti than in Ni, while similar results for chemisorption of H have been observed at the surfaces of both metals.[55] Finally, the Xα-SW method can be used to advantage to remove one uncertainty accompanying ab initio treatments of these systems, namely, restricted flexibility of the basis set. A reliable assessment of the relative contributions of s, p and d functions to bonding requires a flexible basis in order to allow for spatial expansion of orbitals on transfer of electrons from s, p to predominantly d-type molecular orbitals. See Niemczyk and Melius[56] for recent studies showing a favorable comparison between Xα-SW and unrestricted Hartree-Fock treatments.

In order to study the relative contribution of s, p and d functions to bonding, we free all the $(3s)^2$, $(3p)^6$, $(4s)^2$ and $(3d)^2$ electrons from each titanium atom. We only keep $(1s)^2$, $(2s)^2$ and $(2p)^6$ in the frozen core. It is not hard to do the calculation as

long as the cluster size is not big (usually no more than 10 atoms). However, if the cluster size is larger than about ten atoms, the Xα-SW calculation becomes difficult to handle and also time consuming. The primary reason is that the Xα-SW method employs the increment step searching process. As the cluster size increases, the electronic states of each symmetry also increase. The eigenvalues of these electronic states are about the same since they come from the same kind of atom. Therefore, a crowded circumstance of the dense states near any particular eigenvalue is expected. This directly causes a great deal of difficulty in resolving the electronic states at the increment step searching process. The computer may have to spend considerable time in each searching loop and the computation becomes very time consuming and eventually unstable.

From the practical viewpoint, we have to reduce the number of searching loops by reducing the density of the states in a symmetry. One way we can satisfy this requirement is to put more electrons in the core region. However, we also have to make sure that this change does not affect the bonding and charge density. This means that the important physical quantities have to remain the same as electrons are placed in the cores. Therefore, we also perform calculations to check the reliability of results as more electrons are frozen in the core. The first calculation is to include all the $(3\underline{s})^2$ and $(3\underline{p})^6$ of Ti in the core region of Ti_4. The second calculation is to free all the $(3\underline{s})^2$ and $(3\underline{p})^6$ and allow them to participate in the calcu-

lation of the Ti_4 system. By comparing these two results we should be able to determine the role of $(3\underline{s})^2$ and $(3\underline{p})^6$ in bonding and also their effect on the charge density distribution. This information can tell us whether we can proceed to the Ti_{13} calculation by including all the $(3\underline{s})^2$ and $(3\underline{p})^6$ in the core.

III-2 Computation

III-2-1 Geometric Structures of Ti_4 , Ti_7 , and Ti_{13} Clusters

A reasonable choice for the structure of a cluster is to assume a highly symmetrical cluster (e.g. spherical) reflecting the bulk structure and to assume internuclear distances close to the bulk values.[57] Following these guidelines, lattice fragments to be considered are those derived from the hexagonal close-packed structure which is the experimentally determined structure of titanium below 820°C. LEED studies[58] show surface reconstruction but this would not be taken into account in the early stage of this work. These calculation are performed at the titanium metal internuclear distance of 2.95 Å.[59]

The clusters to be considered include a four atom tetrahedral cluster (Ti_4), a seven atom "surface" hexagonal cluster (Ti_7) and a thirteen atom hexagonal close-packed cluster (Ti_{13}). Volume filling clusters are the most appropriate type to use in the SCF-Xα-SW method. The detailed description of these clusters is shown in Figure III-1.

III-2-2 The SCF-Xα-SW Method Applied to Ti_4, Ti_7, Ti_{13} Clusters

The Xα-SW method, its underlying assumptions, procedures and characteristics were described in Chapter I of this dissertation. Results for many systems are available in the literature.[20,23] Here we make note of only those aspects of the method which are of particular relevance to our Ti_x systems in this chapter and Ti_x-H system in Chapter IV. The volume associated with a given system is divided

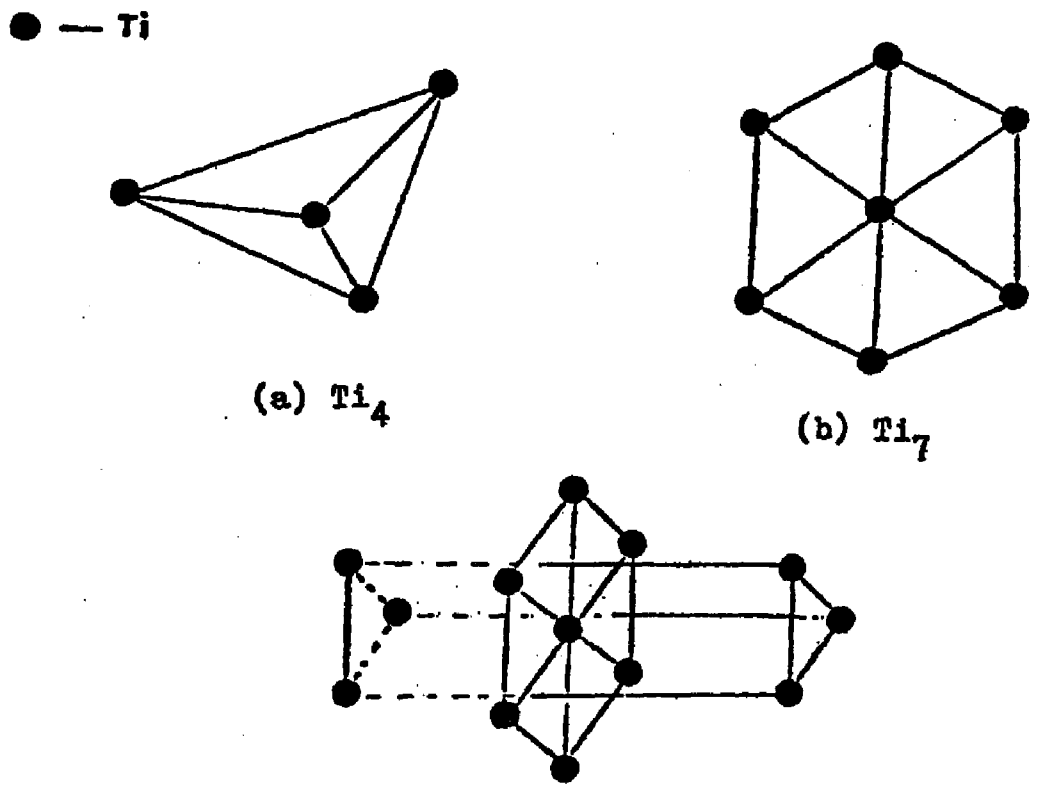

Figure III-1 Three selected titanium clusters: (a) Ti_4 ,(b) Ti_7 ,(c) Ti_{13} .

into atomic, outer-sphere, and interatomic regions. In the muffin-tin approximation, the potential in the interatomic region is assumed to be a constant, while the potential is spherically averaged for the atomic and outer spheres. Matching the boundary conditions and performing some mathematics the radial Schrodinger equation yields a secular equation for the one-electron eigenvalues for each symmetry.

While the free-electron exchange approximation causes the one-electron eigenvalues to have a different interpretation than the usual Hartree-Fock eigenvalues, the two eigenvalue spectra can be correlated without difficulty.[56] On the other hand, the muffin-tin approximation does not allow an accurate calculation of the total energy, but approximate values are nonetheless useful for comparisons of systems with fixed geometries. In addition to the total energy and one-electron energies, the other quantities available from the $X\alpha$-SW calculations are the charges associated with each sphere and the intersphere region, and the percent s, p, d, etc. character for each molecular orbital for each center. The total values of charge in each sphere and total number of s, p, d, etc. electrons in each sphere can also be calculated.

The spheres were chosen to be nonoverlapping. For all the Ti_x and Ti_x-H systems, the virial theorem was satisfied without overlapping the spheres. This result is consistent with those obtained for other transition-metal systems.[23,52,53] The parameters used are given in Table III-1. The exchange parameters used are those derived by Schwarz.[60]

Table III-1 Parameters used in the SCF-Xα-SW calculation on Ti_4, Ti_7, and Ti_{13}. Ti - Ti internuclear distance is 5.5769 a.u.

Xα-SW exchange parameters	Sphere radii (a.u.)
$\alpha_{Ti} = 0.71698$	$R_{Ti}(Ti_4, Ti_7, Ti_{13}) = 2.7885$
$\alpha_{interatomic} = 0.71698$	$R_{outersphere}\ (Ti_4) = 6.2037$ $R_{outersphere}\ (Ti_7) = 8.3654$
$\alpha_{outersphere} = 0.71698$	$R_{outersphere}(Ti_{13}) = 8.3654$

The calculation of a Ti_2 cluster using the Xα-SW method had been published by Fischer and Whitten.[30] The major results of their calculation will be presented here for comparison.

The ratio of the intrasphere volume to the total volume for Ti_2, Ti_4, Ti_7, and Ti_{13} also has been calculated and tabulated in Table III-2.

Table III-2 Volume filling ratio (ratio of the intrasphere volume to the total volume)

	Volume filling ratio
Ti_2	33.3% (~1/3)
Ti_4	48.6% (~1/2)
Ti_7	33.8% (~1/3)
Ti_{13}	92.6% (~9/10)

III-3 Results

III-3-1 Electronic Structure of a Titanium Atom in a Titanium Cluster.

The $(3\underline{d})^3$ $(4\underline{s})^1$ electronic configuration for titanium atoms in bulk titanium has been widely employed in ab initio SCF calculations.[15] However, it has never been proven in sophisticated theoretical calculations that this is the correct atomic configuration to use. The unrestricted SCF-Xα-SW method is capable in principle of carrying out this verification. By calculating the four different systems of Ti_2, Ti_4, Ti_7 and Ti_{13} separately with the aid of the partial-wave feature of the SCF-Xα-SW method, we are able to identify the types of electrons and number of electrons of each type for each atom existing in the cluster. Table III-3 shows the results of the SCF-Xα-SW calculation. Bulk Ti metal has a hexagonal close-packed structure below 820°C.[58] The maximum number of nearest neighbors for a hcp material is twelve. From Tabel III-3, we can clearly see the effect of increasing the nearest neighbors around a titanium atom. As the number of nearest neighbors increases from zero to twelve, the number of $\underline{d}$ electrons per atom in a Ti cluster also increases from 2 to 3.28. The 3.28 $\underline{d}$ electrons per atom is slightly more than 3 $\underline{d}$ electrons per atom which is expected in the bulk Ti metal. However, in our calculation we did not include the second neighbors. These second neighbors can draw some of the electronic charge away from the nearest neighbors and result in less electronic charge density transferring from the nearest neighbors to the designated Ti atom (the one in

Table III-3 Number of d electrons per titanium atom in the cluster for different number of nearest neighbors obtained from the SCF-Xα-SW calculation

	Ti atom	1 N.N.	3 N.N.	6 N.N.	12 N.N.	Bulk Ti
number of d electrons per Ti atom in the cluster	2.00	2.40	2.48	2.87	3.28	3.00*

where N.N. means nearest neighbors

* L. F. Matheiss, Phys. Rev. 134, A970 (1974).

coordinate (0,0,0)). For bulk titanium metal, each Ti atom has 12 nearest neighbors and 6 second neighbors. Therefore, we conclude that the result we get agrees with our prediction. And this calculation once again encourages us to use the $(3\underline{d})^3(4\underline{s})^1$ atomic configuration to treat the inactive Ti atoms which are not near the adsorption sites in the Roothaan-Hartree-Fock SCF-CI calculations. The details are described in Chapter V.

On the surface of a bulk Ti metal, each Ti atom has 9 nearest neighbors. The $(3\underline{d})^3(4\underline{s})^1$ configuration can not be confirmed for surface atoms because our model does not adequately describe a surface atom. The "surface" atoms in our Ti_4 and Ti_{13} clusters do not have 9 nearest neighbors and enough second neighbors. Table III-4 shows the results of our SCF-Xα-SW calculations on the Ti_4 and Ti_{13} systems. In either case, the electronic configuration of each surface Ti atom of our Ti_4 and Ti_{13} clusters will approximately be $(3\underline{d})^{2.4}(4\underline{s})^{1.6}$. This result may be recognized as a good confirmation of our idea $(3\underline{d})^3(4\underline{s})^1$ configuration for the surface atom of a bulk Ti metal considering the in adequacies of the model.

Table III-4 Number of $\bar{d}$ electrons per titanium atom on the surface layer of the Ti_4 and Ti_{13} clusters.

	Ti_4	Ti_{13}
number of $\bar{d}$ electrons per Ti atom on the surface layer of a cluster	2.48	2.38

III-3-2 The Role of the 3s and 3p Electrons in the Titanium Cluster

The M-shell (n=3) contains three subshells, 3s, 3p, and 3d. From atomic theory,[61] we know that the wave function with a lower angular momentum will tend to penetrate further into the nucleus. This property leads to the expected order of occupation 3s, 3p, and 3d. However, a new phenomenon appears in this M shell. This is because the screening effect due to the inner shells of electrons is gradually diminished by the effective charge of the nucleus with increasing atomic number Z. In addition, the energy of the state depends on the total quantum number by a factor of $1/n^2$. These two factors make the energy difference between successive outer shells smaller and smaller. On the other hand, the effects of greater penetration toward the nucleus, by the lower angular-momentum state are becoming larger and larger. There is a point then, at which the low angular-momentum states of the next higher shell may have a lower energy than the higher angular-momentum states of the given shell. This "cross over" first occurs for the 3d subshell and the 4s subshell. The two electrons in the 3d subshell have higher energy than those of the two electrons in the 4s subshell

for a titanium atom. In any case, we treat the two electrons in the 3d and the two electrons in the 4s equally as valence electrons which play a major role in the bonding of a titanium cluster. However, how the two electrons in the 3s subshell and the six electrons in the 3p subshell participate in the bonding of a titanium cluster system is less certain. To check the validity of including 3s and 3p subshell in the core for the larger titanium cluster case (the reasons were described in sec. III-1), calculations for both treating the 3s subshell and the 3p subshell as valence states (calculation A) and including the 3s subshell and the 3p subshell in the core region (calculation B) were carried out. In Table III-5, we show the comparisons. We can easily see the difference between the two cases is less than 1.1% of the energy of any of the occupied 3d and 4s valence states. The 1.1% difference is insignificant. Therefore, we conclude that 3s and 3p subshells can be included in the core without disturbing the bonding valence states - 3d and 4s.

Table III-3 Comparisons between the valence electron eigenvalues of calculation A* and that of calculation B** of Ti_4

* Calculation A - treating $3s^2$ and $3p^6$ as valence states

** Calculation B - including $3s^2$ and $3p^6$ in the core

symmetry of the state	no. of occupied electron	spin	eigenvalues (in Rydberg) calculation A	eigenvalues (in Rydberg) calculation B	difference (in Rydberg) (A - B)
A	1	up	- 0.864	- 0.865	+ 0.001
A	1	down	- 0.705	- 0.705	0.000
A	1	up	- 0.437	- 0.437	0.000
E	2	up	- 0.333	- 0.330	- 0.003
E	2	up	- 0.266	- 0.263	- 0.003
T_1	3	up	- 0.392	- 0.391	- 0.001
T_1	3	up	- 0.336	- 0.334	- 0.002
T_1	3	up	- 0.290	- 0.288	- 0.002
T_2	1	up	- 0.256	- 0.253	- 0.003

III-3-3 d Electron Participation in Bonding

The role of the d electrons in transition metal bonding is still a controversial topic. Therefore, a systematic study should be made. We extend the work further from the earlier studied two- atom cluster to the four- and seven-atom clusters, and then the thirteen- atom cluster. The geometric structures of Ti_2, Ti_4, Ti_7, and Ti_{13} have been discussed in section III-2.

A detailed analysis of the two most active σ bonding orbitals for different size clusters is shown in Table III-6. The partial wave analysis shows an average of about 10% of the d electrons participate in the σ bonding orbitals. However, there is one exception. The exception is that the central atom of the central layer of the Ti_{13} cluster, (i. e. T_1) , has no d electrons involved in the bonding as all bonding electrons are s electrons. This is an interesting result. If we look at the charge distribution, we can see that T_1 of Ti_{13} gives a high percentage of charge to the σ bonding orbitals. Among all the atoms in the four different clusters, the T_1 atom of

Table III- 6 Analysis of Two Most Active Bonding Orbitals in Different Size of Cluster

Cluster	Orbitals	ε_σ (Rydberg)	Charge Distribution					Partial Wave Analysis		
			Q_{out}	Q_{int}	Q_{T_1}	Q_{T_2}	Q_{T_3}	T_1	T_2	T_3
Ti_2	$\sigma_g\uparrow$	-0.344	0.12	0.48	0.20			78s 7p 15d		
	$\sigma_g\downarrow$	-0.272	0.22	0.51	0.14			92s 5p 2d		
Ti_4	$\sigma_g\uparrow$	-0.494	0.07	0.40	0.13			79s 12p 9d		
	$\sigma_g\downarrow$	-0.274	0.12	0.40	0.12			83s 10p 7d		
Ti_7	$\sigma_g\uparrow$	-0.473	0.03	0.42	0.18	0.06		92s 8d	77s 12p 11d	
	$\sigma_g\downarrow$	-0.299	0.02	0.37	0.29	0.05		77s 23d	66s 15p 19d	
Ti_{13}	$\sigma_g\uparrow$	-0.643	0.02	0.36	0.17	0.04	0.03	100s	78s 16p 5d	79s 15p 6d
	$\sigma_g\downarrow$	-0.520	0.01	0.32	0.26	0.04	0.03	100s	68s 20p 12d	67s 19p 14d

Ti_2 and Ti_4 have only one type of titanium atom.

Ti_7 has two different types of titanium atom:

T_1 - one central atom

T_2 - six atoms which surround the central atom

Ti_{13} has three different types of titanium atom:

T_1 - one central atom in central layer

T_2 - six atoms which surround the Ti_1 in the central layer

T_3 - three atoms on top layer plus three atoms on bottom layer

Ti_{13} is the only atom which has twelve nearest neighbors among the four clusters in our calculations. The bulk atom of titanium metal has twelve nearest neighbors and six second neighbors. The second neighbors are not expected to play a significant role in the σ bonding of a bulk atom center since the large distances between them diminish the Coulomb and exchange interactions. Therefore, we can suppose that the T_1 atom of Ti_{13} and the bulk titanium atom may behave in the same manner and have no d and p orbitals participating in bonding between bulk Ti atoms, as many ab initio SCF calculation have suggested. The surface atoms, however, do have considerable d and p-orbital involvement in the metal-metal bonding as many earlier $X\alpha$-SW calculations have concluded. Thus, we reviewed those calculations once again and found that all the atoms involved in the earlier $X\alpha$-SW calculations are surface atoms.

The p orbital is not present in the T_1 atom of Ti_{13}, nor in the T_1 atom of Ti_7. These two atoms are well surrounded by other types of titanium atoms. The surface atoms have increasing p orbital participation in the bigger clusters. The percentage of p orbital participation in the two most active σ bonds of surface atoms are 6%, 11%, 13%, and 18% for Ti_2, Ti_4, Ti_7, and Ti_{13} respectively. Of course s orbitals on neighboring centers can result in p-like orbital bonding on a given center.

It should be further noted for this analysis of two most active σ bonding orbitals, that the charge leaking out to the outersphere region decreases from 0.17e for Ti_2, through 0.1e for Ti_4 and 0.03e

for Ti_7, to 0.01e for Ti_{13}. This means that bonding takes place only inside the cluster if the cluster size is larger than thirteen titanium atoms.

III-3-4 Systematic Study on the Average Spin Magneton Number Per Atom for Different Size of Ti Clusters.

A titanium atom has a spin magneton number of two, while titanium metal has an average spin magneton number per atom of zero, because titanium is a non-magnetic material. It is interesting to study why this occurs. The unrestricted SCF-Xα-SW method is capable of providing the necessary information for this research. Slater, et al.[20] used this method to calculate the average spin magneton number per atom of a vanadium cluster. They concluded that the average spin magneton number per atom depends on the parameter-lattice constant. The smaller the lattice constant, the less the average spin magneton number per atom. However, we chose cluster size, rather than lattice constant as our variable. After all, the formation of a metal occurs as an accretion of individual atoms. The size of a cluster can be changed freely and treated as a variable. Therefore, we present the calculation of four different size clusters - Ti_2, Ti_4, Ti_7, and Ti_{13} in this spin magneton number study. Table III-7 shows the results of the SCF-Xα-SW calculations. The average spin magneton number per atom first increases from 3 for Ti_2 to 3.5 for Ti_4, then decreases to 3.1 for Ti_7 and 2.5 for Ti_{13}. The Ti_4 tetrahedral cluster has a maximum average spin magneton number per atom. This probably has

Table III-7 Average spin magneton number per atom for different size titanium clusters by the SCF-Xα-SW calculation

	Ti atom	Ti_2	Ti_4	Ti_7	Ti_{13}	Bulk Ti
average spin magneton number per atom	2.00	3.00	3.50	3.10	2.50	0.00

to do with the unfavorably high orbital energy of the β spin states for the Ti_4 cluster as shown in Figure III-2. If the energies of those β spin orbitals are too high above the Fermi level, most valence electrons will be forced to occupy the relatively lower energy α spin orbitals. However, this phenomenon is slightly different in the Ti_7 and Ti_{13} clusters. The nature (i.e. geometry, bonding, etc.) of these two clusters is such that the energy splitting between the α and β spins is smaller than that of the Ti_4 cluster (see Figure III-2). From this we can expect that some more β-spin orbitals lie below the Fermi level and should be occupied. The energy splitting between opposite spins of the Ti_{13} cluster is the smallest among the four clusters (Ti_2, Ti_4, Ti_7, and Ti_{13}). Therefore, we have evidence to predict that increasing the size of a cluster (>13 atoms) should reduce the average spin magneton number per atom in a bigger cluster. And as the size of a titanium cluster increases, the average spin magneton number per atom of the whole cluster presumably approaches zero.

III-3-5 Total Energy Per Atom in Different Size of Titanium Clusters and Prediction of Bonding.

Fischer and Whitten[30] studied Ti chains. They concluded that the SCF-Xα-SW method is suitable for the study of electronic structure of transition metal clusters provided that the total energy is only considered for different states with fixed geometry. The muffin-tin

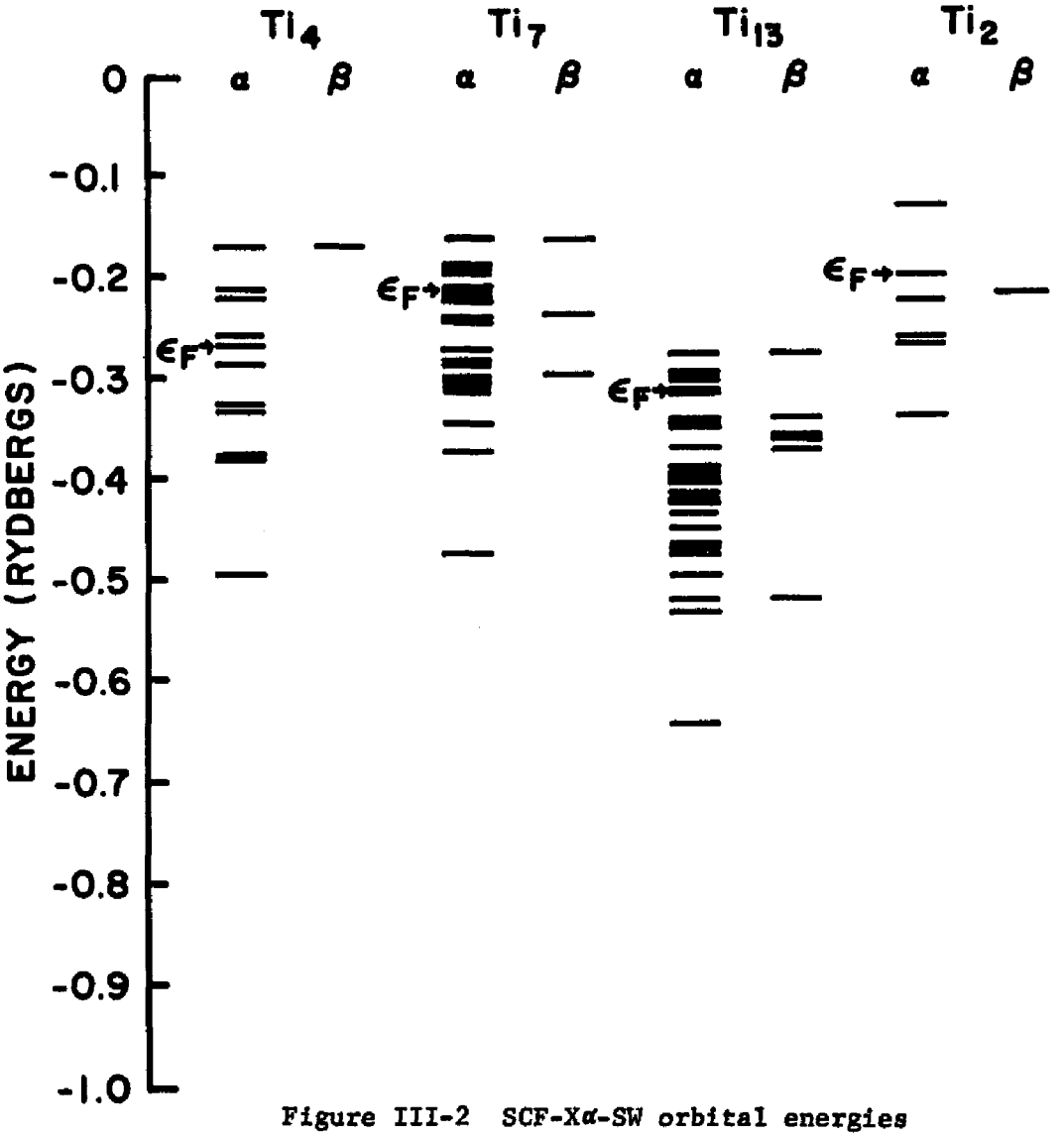

Figure III-2 SCF-Xα-SW orbital energies of Ti_2, Ti_4, Ti_7, and Ti_{13} clusters.

approximation employed in this study does not presently allow for accurate calculation of activation barriers and dissociation energies. However, our new studies show that the total energies per atom of several different geometries may still be useful to predict the relative bonding of different size clusters qualitatively.
Table III-8 tells us that the Ti_{13} system gives the lowest relative total energy per atom and thus shows that the Ti_{13} system has the highest bonding energy among the systems.

From Table III-8, we see that the total energy per atom is lowered from -1696.79 Rydbergs for Ti_2 to -1696.96 Rydbergs for Ti_{13}. Ti_2 and Ti_7 have the same total energy per atom. Ti_2 is a two atom cluster and Ti_7 is a seven atom "surface" hexagonal cluster. The volume filling ratios of both cases are low, 33.3% for Ti_2 and 33.8% of Ti_7. This low ratio also gives a less negative intersphere constant potential as shown in Table III-8. One of the SCF-Xα-SW procedures is to match the boundary conditions at the atomic- and outer- sphere boundaries. This less negative intersphere constant potential could in turn give less negative energy states (see Figure III-2) and a less negative total energy per atom. The lowest relative total energy per atom of Ti_{13} is meaningful because each of the structures(Ti_2, Ti_4, Ti_7, and Ti_{13}) may be viewed as a small part of titanium metal crystals. Therefore, our calculated results may indicate that the bulk Ti metal tends to form a stable system.

Table III-8 Total energy per atom, volume filling ratio and constant potential for different size clusters

		Ti_2	Ti_4	Ti_7	Ti_{13}
Total energy per atom (in Rydberg)		-1696.79	-1696.91	-1696.79	-1696.96
Volume filling ratio (in %)		33.3	48.6	33.8	92.6
Constant potential (in Rydberg)	spin down	-0.4299	-0.5658	-0.4167	-0.6694
	spin up	-0.3367	-0.3474	-0.2237	-0.5088

Ti_2 - two atom linear cluster

Ti_4 - four atom tetrahedral cluster

Ti_7 - seven atom "surface" hexagonal cluster

Ti_{13} - thirteen atom hexagonal close-packed cluster

Volume filling ratio - the ratio of the intrasphere volume to the total volume

III-3-6 Comparison of SCF-Xα-SW Calculations with Feibelman's Band Structure Calculations on Ti.

Feibelman, et al.[62] studied the electronic structure of a thin (11-layer) Ti(0001) film. They used a numerical method based on a linear combination of Gaussian orbitals to carry out their calculations. The only approximation they made is the assumption of a local exchange-correlation potential. The result of their calculation is shown in Figure III-3. They found that the density of states (DOS) in the lower d-band region narrows dramatically at the surface. This is due primarily to a quite narrow band of surface states found to coincide with the Ti Fermi energy, extending no more than a few tenths of an eV on either side of it. This result suggests that occupation of the surface band plays a large role in determining the strength of the dipole layer at the Ti surface, and hence the Ti(0001) work function. The work function they found is 3.8 eV, in good agreement with the experimental result, 3.95 eV.[63] The other major result is that the surface DOS for Ti(0001) is strongly modified in the lower portion of the d band. In the bulk, the Fermi level lies at a minimum between two peaks in the DOS, while at the surface these peaks appear to merge and sharpen, with the new maximum falling just at E_F, as shown in Figure III-3.

We performed SCF-Xα-SW calculation on three different clusters, namely, Ti_4, Ti_7, and Ti_{13}. The results of our calculation are shown in Figure III-4, Figure III-5, and Figure III-6. We see that

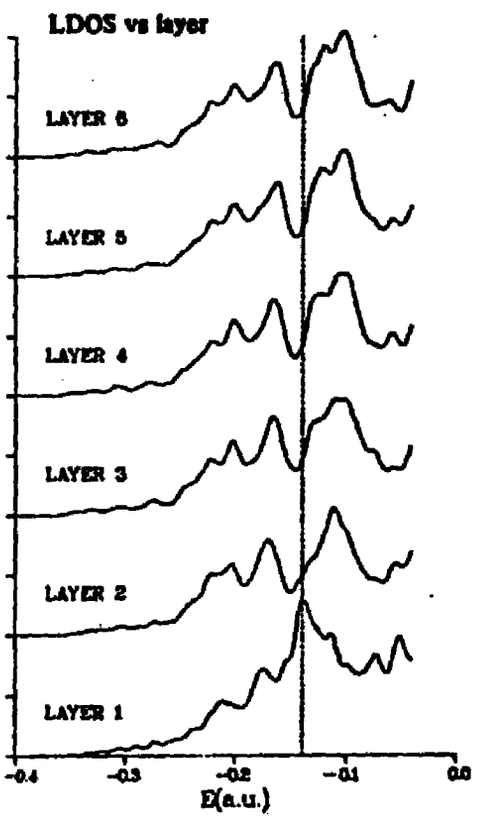

FIG.III-3Layerwise local density of states (LDOS) for an 11-layer Ti(0001) film. The vacuum level is at energy 0.0. The dotted line indicates the Fermi level at $E = -0.139$ a.u. ($= -3.8$ eV). Note the strong surface resonance in the outermost ("1st") layer.

Figure taken from: P.J. Feibelman, J.A. Appelbaum and D.R. Hamann, Phys. Rev. B20, 1433 (1972).

the DOS of Ti_4 and Ti_7 clusters resemble the DOS of layer 1 of Feibelman's 11 layer Ti(0001) film and perhaps both may be compared with a surface layer of Ti metal. On the contrary, the DOS of the Ti_{13} cluster has features similar to the DOS of layer 6 of the 11 layer Ti(0001) film. The phenomena which appeared in the Feibelman's data do appear again in our calculation. We see the narrow $\underline{d}$ band of surface states in Ti_4 and Ti_7. And we also see that the Fermi level of Ti_{13} lies at a minimum between two peaks in the DOS, while these peaks in Ti_4 and Ti_7 clusters appear to merge and sharpen, with the new maximum falling just at E_F as shown in Figure III-4, Figure III-5, and Figure III-6. On the other hand, we get three different work functions for three different clusters. The work functions are 3.6 eV, 3.0 eV, and 4.2 eV for Ti_4, Ti_7, and Ti_{13} respectively. Since the Ti_7 cluster has a low volume filling ratio (33.8%) and the muffin-tin approximation was employed in this calculation, the 3.0 eV of work function for Ti_7 cluster is especially unreliable. The Ti_{13} cluster has high volume filling ratio (92.6%). Therefore, the work function of Ti_{13} cluster, 4.2 eV, can be considered a reasonable result, in agreement with experiment.

III-3-7 The Relationship between Total Energy and Singly Occupied Orbitals for Ti_4 cluster.

During the course of interaction between the adsorbate and the lattice in a chemisorption process, we expect that the atoms of the

Figure III-4 Density of states for Ti_4 cluster.
The Fermi energy is indicated by a dashed line.

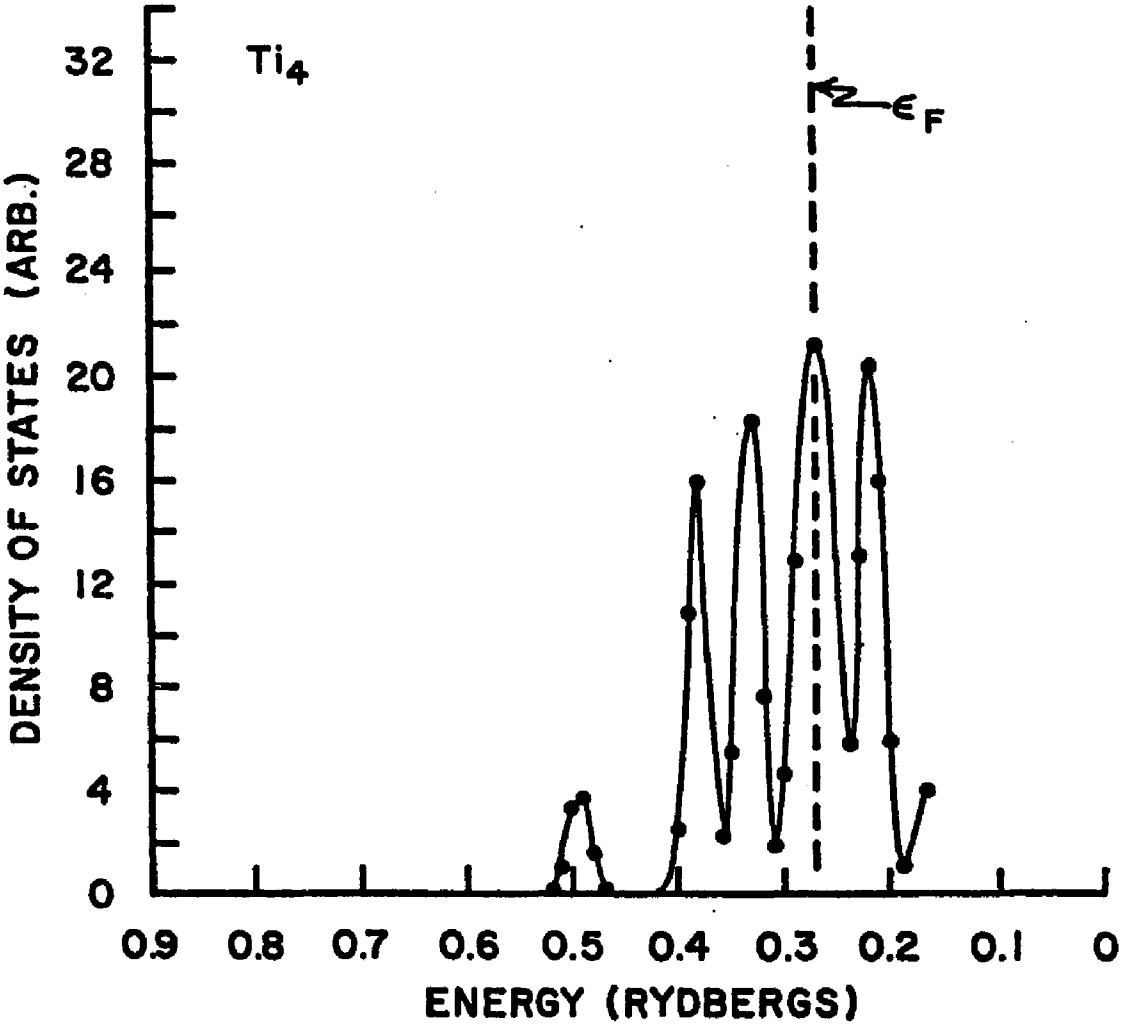

Figure III-5 Density of states for Ti_7 cluster. The Fermi energy is indicated by a dashed line.

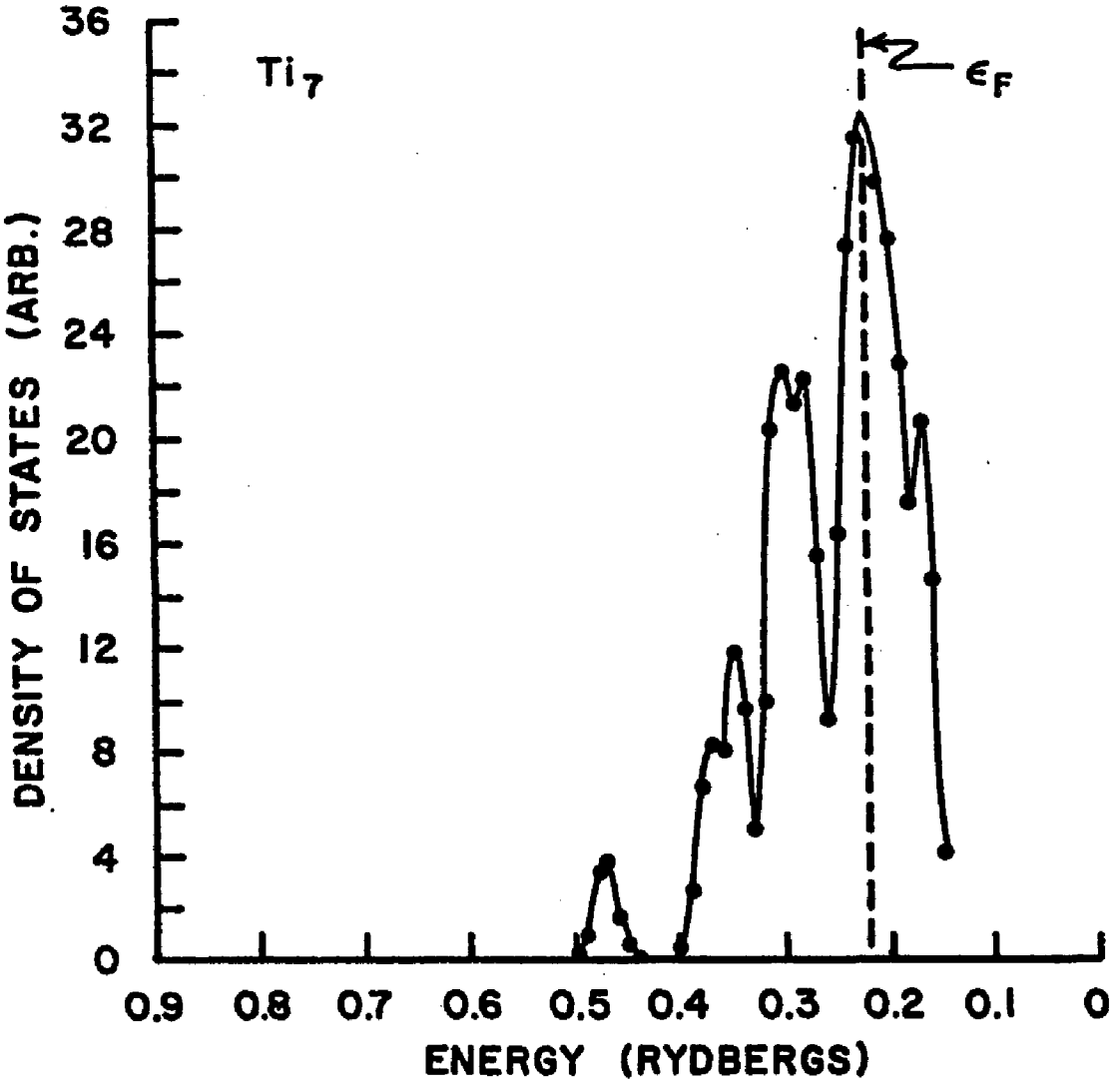

Figure III-6 Density of states for Ti_{13} cluster. The Fermi energy is indicated by a dashed line.

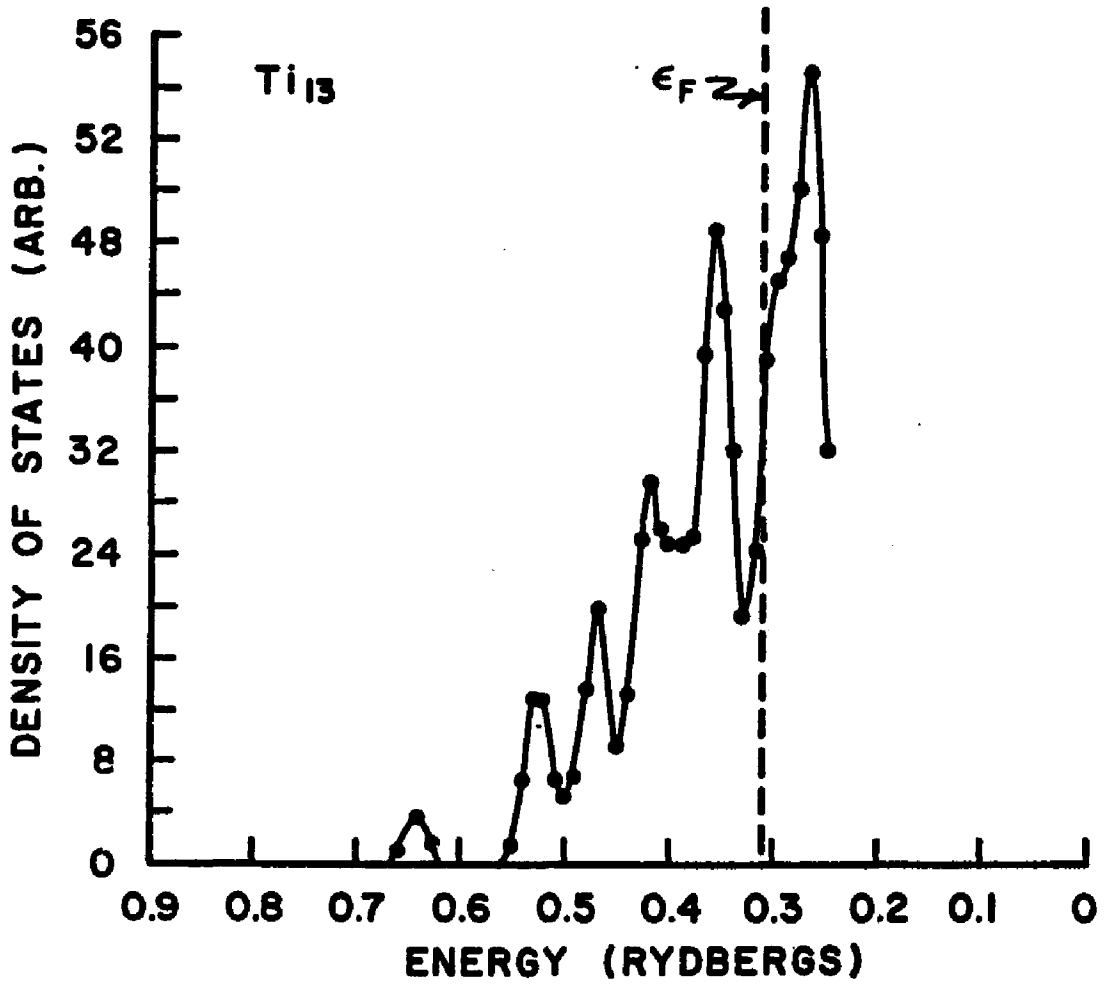

lattice near the adsorbate are more important than the rest of the lattice. This is mainly because the Coulomb and exchange interactions are stronger in a shorter range. Therefore, it is essential to study the intrinsic electronic arrangement of the few atoms which geometrically touch the adsorbate atoms. Ti_4 cluster is a good example for studying this aspect since it provides the information for the three Ti atoms on the lattice surface, touching one of the adsorbate atoms. The calculated results of the Ti_4 low lying states are listed in Table III-9. The data show that the different choices of singly occupied a_1, a_2, e, t_1, and t_2 orbitals for valence electrons give various total energies. Here, a_1, a_2, e, t_1, and t_2 are the five representations of the T_d point group which the Ti_4 cluster belongs to. We identify the character of the orbitals by looking at the computer generated partial-wave analysis as shown in Table III-10. We find that the $1a_1$ orbital is s-like while the rest of the orbitals are d-like. State I (see Table III-9) has the lowest energy among the listed states. The data also indicate that the s-like orbital of State I is doubly occupied and the d-like orbitals of State I are singly occupied. Attempts to singly occupy the s-like orbital and doubly occupy the d-like orbitals do not lower the total energy (see from State II to State VII in Table III-9). Thus, we conclude that the singly occupied d-like orbitals can lower the total energy of Ti_4 cluster.

Table III-9 Ti_4 low-lying states. Results correspond to different choices of singly occupied a_1, a_2, e, t_1, and t_2 orbitals. Unit of the total energies is in Rydbergs.

State		Total Energy
I	$(1a_1\uparrow)(1a_1\downarrow)(2a_1\uparrow)$ $(1e\uparrow\uparrow)(2e\uparrow\uparrow)$ $(1t_1\uparrow\uparrow\uparrow)(2t_1\uparrow\uparrow\uparrow)(3t_1\uparrow\uparrow\uparrow)$	-6787.621
II	$(1a_1\uparrow)(1a_1\downarrow)(2a_1\uparrow)$ $(1e\uparrow\uparrow)(2e\uparrow\uparrow)$ $(1t_1\uparrow\uparrow\uparrow)(1t_1\downarrow)(2t_1\uparrow\uparrow\uparrow)(3t_1\uparrow\uparrow\uparrow)$	-6787.551
III	$(1a_1\uparrow)(1a_1\downarrow)(2a_1\uparrow)$ $(1e\uparrow\uparrow)(2e\uparrow\uparrow)$ $(1t_1\uparrow\uparrow\uparrow)(1t_1\downarrow)(2t_1\uparrow\uparrow\uparrow)(3t_1\uparrow\uparrow)$	-6787.527
IV	$(1a_1\uparrow)(2a_1\uparrow)$ $(1e\uparrow\uparrow)(2e\uparrow\uparrow)$ $(1t_1\uparrow\uparrow\uparrow)(1t_1\downarrow)(2t_1\uparrow\uparrow\uparrow)(3t_1\uparrow\uparrow\uparrow)$	-6787.520
V	$(1a_1\uparrow)(2a_1\uparrow)(3a_1\uparrow)$ $(1e\uparrow\uparrow)(2e\uparrow\uparrow)$ $(1t_1\uparrow\uparrow\uparrow)(2t_1\uparrow\uparrow\uparrow)(3t_1\uparrow\uparrow\uparrow)$	-6787.465
VI	$(1a_1\uparrow)(1a_1\downarrow)$ $(1e\uparrow\uparrow)(2e\uparrow\uparrow)$ $(1t_1\uparrow\uparrow\uparrow)(1t_1\downarrow)(2t_1\uparrow\uparrow\uparrow)(3t_1\uparrow\uparrow\uparrow)$	-6787.441
VII	$(1a_1\uparrow)(1a_1\downarrow)(2a_1\uparrow)$ $(1e\uparrow\uparrow)(1e\downarrow\downarrow)$ $(1t_1\uparrow\uparrow\uparrow)(2t_1\uparrow\uparrow\uparrow)(3t_1\uparrow\uparrow\uparrow)$	-6787.402

where a_1, a_2, e, t_1, and t_2 are the five representation of the T_d point group.

Table III-10 Partial-wave analysis of the valency orbitals of the Ti_4 cluster. Only the valency orbitals of State I (see Table III-9) are presented here.

Orbital	ϵ (in Rydbergs)	Partial-wave analysis (%) (titanium atomic region)		
$1a_1$ ↑	-0.494	79s	12p	9d
$1a_1$ ↓	-0.274	83s	10p	7d
$2a_1$ ↑	-0.382		3p	97d
1e ↑↑	-0.332		2p	98d
2e ↑↑	-0.267		2p	98d
$1t_1$ ↑↑↑	-0.381	16s	7p	77d
$2t_1$ ↑↑↑	-0.335	4s		96d
$3t_1$ ↑↑↑	-0.286	4s	3p	93d

III-3-8 The Role of the Constant Potential Related to the d Electron Participation in Ti-Ti σ Bonding in Ti_2, Ti_4, Ti_7, and Ti_{13} Clusters.

Fischer and Whitten[30] carried out electronic structure calculations of TiH and Ti chains using the Xα-SW method. They pointed out that the amount of d-wave contribution to the σ electrons seems to depend on the value of the constant potential. Thus, the d electron population per Ti center increases as the depth of the constant potential increases. However, this conclusion was based on the results obtained from non-self-consistent-field calculations. We reexamined this statement by studying the four different titanium clusters - Ti_2, Ti_4, Ti_7, and Ti_{13}. The geometric structures of the Ti_4, Ti_7, and Ti_{13} clusters were described in Sec. III-2. Ti_2 of course has a linear structure. All the calculations were done by the self-consistent-field Xα-SW method.

Our calculated results are listed on Table III-11. The data show that the value of the constant potential does not have any significant effect on determining the d electron population per Ti center. A large value of the constant potential does not necessarily lead to a large d electron population per Ti center. For instance, the magnitude of the constant potential of the Ti_4 cluster (0.35 a.u. for α spin and 0.57 a.u. for β spin) is larger than that of Ti_7 cluster (0.22 a.u. for α spin and 0.42 a.u. for β spin). On the contrary, the d electron population of the Ti_4 cluster (2.48 e) is smaller than that of Ti_7 cluster (either 2.87 e for T_1 atom or

Table III-11 Constant potential, d electron population per Ti center, and Fermi energy of Ti_2, Ti_4, Ti_7, and Ti_{13} clusters.

		Ti_2	Ti_4	Ti_7	Ti_{13}
Constant potential (in a.u.)	α spin	-0.34	-0.35	-0.22	-0.51
	β spin	-0.43	-0.57	-0.42	-0.67
Number of d electron per Ti center	T_1	2.40	2.48	2.87	3.28
	T_2			2.68	2.43
	T_3				2.38
Fermi energy (in eV)		3.00	3.60	3.00	4.20

where T_1, T_2, and T_3 were described in Table III-6.

2.68 e for T_2 atom). The Ti_7 cluster has two types of atoms, T_1 and T_2 which were described in Table III-6.

On the other hand, we found that the value of the constant potential is closely related to the Fermi energy of a cluster. The Fermi energy of a cluster is directly associated with the work function of the metal. Our results show proportionality between the Fermi energy and the value of the constant potential. The Ti_{13} cluster has the highest value of the Fermi energy (4.2 eV) and it has the largest value of the constant potential among the four investigated clusters. Ti_2 and Ti_7 have the same magnitude of the Fermi energy (3 eV) and both clusters have about the same value for the constant potential.

CHAPTER IV

CALCULATION OF CHEMISORPTION OF HYDROGEN ON Ti(0001) USING THE Xα-SW METHOD

IV-1 Introduction

Chemisorption of hydrogen on metal surfaces is an important problem. We list three reasons for choosing to study the chemisorption of hydrogen on a titanium surface. The first reason is that hydrogen could possibly become an important energy source[64] in the near future. A safe and highly efficient method of hydrogen storage is not yet known. Recently, several reports[55,65] have pointed out that the transition metals and their alloys are potential hydrogen storage systems. Ti forms a bulk hydride and the reaction of H with Ti surfaces determines the uptake of H in a hydrogen storage application.[65] However, the study is still in the preliminary stage and further research is definitely needed from a practical viewpoint. Secondly, a basic understanding of chemisorption and catalysis is lacking at the molecular level. Hydrogen is the simplest element. It is certainly a good choice to use hydrogen in this study for reducing the complexity of the problem. In the mean time, from the theoretical point of view titanium is one of the easier first row transition metal elements to deal with, since the intrashell correlation energy for the 3d electrons is not expected to be as important as it is in the case of Ni and other transition metals with more than half filled d shells.[30] Moreover, a number of experiments on titanium surfaces

with known configurations are available.[58] This information strongly encouraged us to do this research. Finally, the titanium-hydrogen system is important because Ti is a technologically important material and because H is a common impurity in it.[66] Ti also reacts readily with H making it the single most important getter material for H.[67]

Here we use the SCF-Xα-SW method to study the electronic structure of three different titanium-hydrogen systems, namely, HTi_4, Ti_4H and $Ti_{13}H_2$. The detailed descriptions of these three systems are presented in the next section (IV-2). The calculations are aimed at clarifying the relevant bonding properties of the titanium-hydrogen system. The determination of these bonding properties is a major step in building a theory of chemisorption.

In 1979 Fischer and Whitten carried out SCF-Xα-SW calculations on titanium chains and titanium hydride. One of the major conclusions of their studies is that the SCF-Xα-SW method is suitable for the study of the electronic structure of transition metal clusters provided that the total energy is only considered for different states with fixed geometries. Thus the muffin-tin approximation employed in their work does not allow for accurate calculation of activation barriers and dissociation energies. The muffin tin approximation is also employed here due to its rapid convergence. Of course, the same total energy deficiency appears in our calculation too. Fortunately, the SCF-Xα-SW method proved to give a

useful description of the eigenenergies for a given system. After a suitable density of states calculation, these eigenenergies yield an energy spectrum for the system. By making a comparison between this calculated energy spectrum and the experimental UPS data, we may be able to gain some information about the geometry of the titanium-hydrogen system.

IV-2 Computation

The clusters to be considered for the titanium-hydrogen systems include a four atom tetrahedral titanium cluster with a hydrogen atom in the center (HTi_4), a four atom tetrahedral titanium cluster with a hydrogen atom at the hcp site (Ti_4H) and a three layer thirteen atom hexagonal closed-packed titanium cluster with two hydrogen atoms in the two hcp sites on both top and bottom layers ($Ti_{13}H_2$). Figure IV-1 shows the three selected titanium-hydrogen clusters. The parameters and the radii of spheres used in the SCF-Xα-SW calculation on HTi_4, Ti_4H and $Ti_{13}H_2$ are tabulated in Table IV-1.

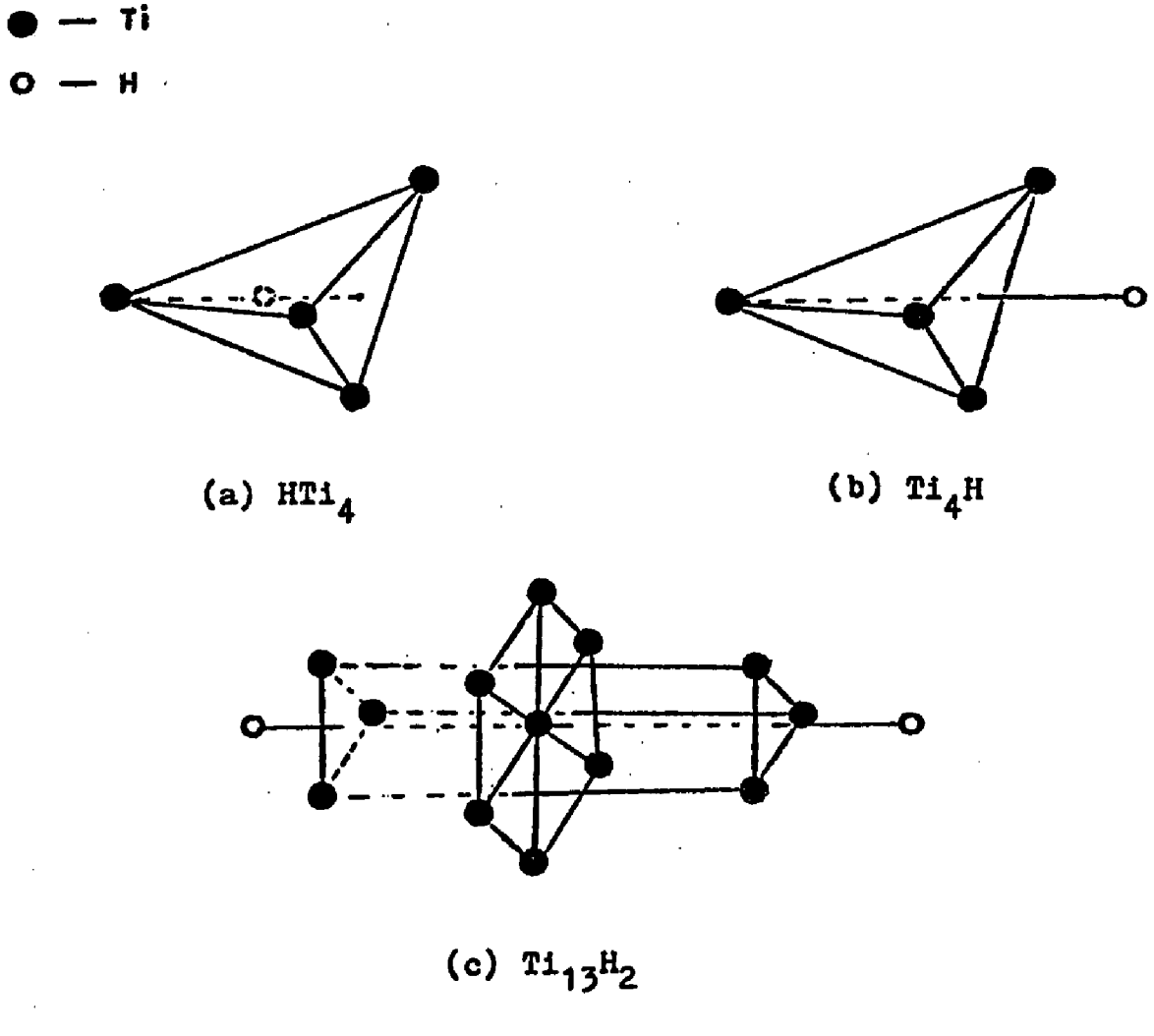

Figure IV-1 Three selected titanium-hydrogen clusters: (a) HTi_4 ,(b) Ti_4H and (c) $Ti_{13}H_2$.

Table IV-1 Parameters used in the SCF-Xα-SW calculation on HTi_4, Ti_4H, and $Ti_{13}H_2$. Ti-H and Ti-Ti internuclear distances are 3.7885 a.u. and 5.5769 a.u. respectively.

	Xα-SW exchange parameters	Sphere radii (a.u.)
	α_{Ti} = 0.71698	R_{Ti} = 2.7885
	α_{H} = 0.77725	R_{H} = 1.000
HTi_4:	$\alpha_{outersphere}$=0.71766	$R_{outersphere}$=6.2037
	$\alpha_{intersphere}$=0.71766	
Ti_4H:	$\alpha_{outersphere}$=0.71766	$R_{outersphere}$=6.2037
	$\alpha_{intersphere}$=0.71766	
$Ti_{13}H_2$:	$\alpha_{outersphere}$=0.71701	$R_{outersphere}$=8.3655
	$\alpha_{intersphere}$=0.71701	

IV-3 Results

IV-3-1 The Role of the d Orbitals in the Bonding of the H Atom to the Titanium Cluster

Configuration-interaction calculations on TiH indicated a limited role for the d electrons in the Ti-H bond.[49,50] In contrast to this result, Xα-SW calculations by Messmer, et al.[52] of H-atom interactions with Ni, Pd, and Pt clusters indicate a strong role for the d orbitals in the bonding of a H atom to the surface of the transition-metal cluster. Fischer and Whitten also used the Xα-SW method to carry out TiH and Ti chain calculations and concluded that many of the σ levels in TiH and Ti_2 exhibit a great deal of d function participation. Since all of the above calculations involved hydrogen on the surface of the transition-metal clusters, we suppose that the presence of the H atom could change some characteristics of the bonding between the transition-metal atoms. Thus, we carried out another Xα-SW calculation on the chemisorption of hydrogen on Ti(0001) to obtain a more thorough understanding of the d function participation in bonding.

We have studied the electronic structures of Ti_4, Ti_7, and Ti_{13} clusters in Chapter III. We know that the two most deeply bound σ bonding orbitals in those Ti clusters contain about 10% of the d participation with the exception of the T1 of the Ti_{13} cluster. Here we do further calculations on the HTi_4, Ti_4H, and $Ti_{13}H_2$ clusters. We list the calculated results of the two most deeply bound σ bonding orbitals of Ti_4, HTi_4, and Ti_4H in Table IV-2. Comparable results

Table IV-2 Partial-wave analysis on the two most deeply bound σ bonding orbitals for Ti_4, HTi_4, and Ti_4H clusters.

Case	Orbital	ϵ_σ (Ryds.)	Partial-Wave Analysis (%) T1	T2
Ti_4	$\sigma\uparrow$	-0.494	79s 12p 9d	
	$\sigma\downarrow$	-0.274	83s 10p 7d	
HTi_4	$\sigma\uparrow$	-0.864	31s 28p 41d	
	$\sigma\downarrow$	-0.705	28s 29p 43d	
Ti_4H	$\sigma\uparrow$	-0.689	55s 23p 21d	43s 23p 34d
	$\sigma\downarrow$	-0.524	46S 26P 27d	37s 25s 39d

where

T1 of Ti_4H - the only Ti atom which does not touch the H atom.

T2 of Ti_4H - any of the three Ti atoms which touch the H atom.

Ti_4 and HTi_4 have only one type of Ti atoms-T1.

for Ti_{13} and $Ti_{13}H_2$ are tabulated in Table IV-3. The data of Table IV-2 show a stronger $\underline{d}$ participation in the two most deeply bound σ bonding orbitals of HTi_4 and Ti_4H than those of Ti_4. The 42% $\underline{d}$ participation for HTi_4 is compared to 8% $\underline{d}$ participation for Ti_4. The analysis of the Ti_4H case is more complicated. This is because Ti_4H has two different types of Ti atoms - T1 and T2. T1 of Ti_4H is the Ti atom which touches the other three Ti atoms and is furthest from the H atom (see Figure IV-1(b)). T2 of Ti_4H represents any of the three atoms which directly touch the H atom. From Table IV-2, it is seen that the $\underline{d}$ participation in the two most deeply bound σ bonding orbitals for the T2 atom of Ti_4H are stronger than those of the T1 atom of Ti_4H, 24% for T1 compared to 37% for T2. In HTi_4 and Ti_4H systems, the single electron of the hydrogen is embedded in the 88 electrons of the four Ti atoms. The electronic charge of the hydrogen atom is only 1.1% of the electronic charge of the four Ti atoms. Therefore the 13% difference of $\underline{d}$ participation in the two most deeply bound σ bonding orbitals between the T2 and T1 of Ti_4H is meaningful. A similar result is given for $Ti_{13}H_2$ in Table IV-3. The $Ti_{13}H_2$ has three types of Ti atoms - T1, T2, and T3. T1 of $Ti_{13}H_2$ is the central Ti atom in the central layer. T2 of $Ti_{13}H_2$ is any of the six atoms surrounding T1 in the central layer. T3 of $Ti_{13}H_2$ represents any of the six atoms touching the two H atoms (see Figure IV-1(c)). T3 of $Ti_{13}H_2$ has 32% $\underline{d}$ participation on the two most deeply bound σ bonding orbitals as opposed to 12% for T1 and 3% for T2. In the $Ti_{13}H_2$ cluster, the two electrons of the two hydrogen atoms carry

Table IV-3 Partial-wave analysis of the two most deeply bound σ bonding orbitals for Ti_{13} and $Ti_{13}H_2$ clusters. Orbital energies in Rydbergs.

Case	Orbital	ϵ_σ	Partial-Wave analysis (%) T1	T2	T3
Ti_{13}	$\sigma\uparrow$	-0.644	100s	79s 16p 5d	79s 15p 6d
	$\sigma\downarrow$	-0.520	100s	68s 20p 13d	67s 19p 14d
$Ti_{13}H_2$	$\sigma\uparrow$	-0.738	91s 9d	83s 16p 2d	50s 18p 32d
	$\sigma\downarrow$	-0.637	85s 15d	78s 19p 3d	47s 21p 32d

where

T1- The central Ti atom of the central layer.
T2- Any of the six Ti atoms which touch T1 and are in the central layer (see Fig.IV-1).
T3- Any of the six Ti atoms in the top and the bottom layer.

T3 of the $Ti_{13}H_2$ cluster touches the H atom (see Fig. IV-1).

only 0.3% of the electronic charge of the thirteen Ti atoms. Therefore any effect due to the presence of the hydrogen atoms is expected to be smaller than that in the Ti_4H case. Therefore, the above differences between T3 and T1 of $Ti_{13}H_2$ are significant. This indicates that the H atom plays an essential role in enhancing the d function participation in the two most deeply bound σ bonding orbitals of its nearest neighbor Ti atoms. Table IV-4 shows the total charge density analysis of the Ti_4, HTi_4, and Ti_4H clusters. Again we see that the d electronic charge of T2 is more than the d electronic charge of T1 by 0.1 extra electron (2.61 d electrons for T2, and 2.51 d electrons for T1 of the Ti_4H case). The total charge per T2 atom of Ti_4H is 20.98 electrons while the total charge per T1 atom of Ti_4H is 20.81 electrons. This indicates a small amount of charge transfer among the Ti atoms through the introduction of an H atom on the Ti surface. This also implies that the bonding of the Ti atoms is no longer purely metallic, but that an ionic component for atoms participating in the chemisorption bonding has been added to it.

A similar result for $Ti_{13}H_2$ is shown in Table IV-5. By comparing the data of Ti_{13} and $Ti_{13}H_2$, we see that the T3 atom, which touches the H atom in the $Ti_{13}H_2$ case, increases the d electronic charge from 2.38 e for Ti_{13} to 2.45 e for $Ti_{13}H_2$. Also the total charge per T3 atom increases from 20.84 e for Ti_{13} to 20.95 e for $Ti_{13}H_2$, while the total charge per T2 atom decreases from 20.99 e for Ti_{13} to 20.90 e for $Ti_{13}H_2$. The above changes of the d electronic charge are about

Table IV-4 Total charge density analysis of the Ti_4, HTi_4, and Ti_4H clusters.

Case	T1	T2
Ti_4	6.33s 12.07p 2.48d Total charge per T1 atom = 20.88 e	
HTi_4	6.26s 12.13p 2.61d Total charge per T1 atom = 21.01 e	
Ti_4H	6.22s 12.07p 2.51d Total charge per T1 atom = 20.81 e	6.26s 12.11p 2.61d Total charge per T2 atom = 20.98 e

where
T1 and T2 of Ti_4H were described in Table IV-2.

Table IV-5 Total charge density analysis of the Ti_{13} and $Ti_{13}H_2$ clusters.

Case	T1	T2	T3
Ti_{13}	6.57s 12.47p 3.28d Total charge per T1 atom= 22.35 e	6.39s 12.17p 2.43d Total charge per T2 atom= 20.99 e	6.32s 12.14p 2.38d Total charge per T3 atom= 20.84 e
$Ti_{13}H_2$	6.56s 12.48p 3.24d Total charge per T1 atom= 22.32 e	6.38s 12.17p 2.36d Total charge per T2 atom= 20.90 e	6.32s 12.18p 2.45d Total charge per T3 atom= 20.95 e

where
T1, T2, and T3 were described in Table IV-3.

0.1 e which is usually considered a small amount. However, this amount is produced by the 0.3% electronic charge participation of the two hydrogen atoms. Thus, we consider the 0.1 e change meaningful. The above analysis suggests that the H atom tends to increase the d participation in the bonding of a Ti_xH cluster, and also changes the nature of the Ti - Ti bonding in chemisorption from pure metallic to a metallic-ionic mixed bonding.

IV-3-2 Determination of the Surface Geometry of the Titanium-Hydrogen System.

The determination of adsorption geometries via low-energy-electron diffraction (LEED)[68] has been considerably improved recently. Other types of scattering techniques[69,70,71] have also progressed. However, it is still far from routine to determine the location of the atoms at a surface. This statement is particularly true for surface hydrogen atoms, since H is a weak electron scatterer. For example, Feibelman and Hamann[66] extended their studies by using angle-resolved photoemission spectroscopy which is sensitive to surface atomic arrangement, and thus can be used to narrow down possible surface geometries. They also used the self-consistent linear-combination-of-atomic-orbitals (SC-LCAO) method to calculate the surface band structure for each of five different symmetry sites for H on the Ti surface as shown in Figure IV-2. They found that both the position of the H peak (5 eV below E_F) and the changes in d bands of Ti(0001) induced by the H

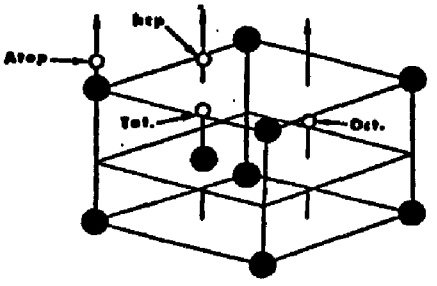

FIG. IV-2 Schematic of the unit cell of a basal-plane hcp film. The Ti atoms are represented by closed circles. The sites tried for the H adlayer are indicated, including the atop (onefold) site, a threefold "hcp" site, the tetrahedral underlayer site, and the octahedral site.

Figure taken from : P. J. Feibelman and D. R. Hamann
Phys. Rev. B21, 1385 (1980).

layer were strongly dependent on the assumed surface geometry. They also found that locating the H's in the three-fold sites, 0.8 a.u. outside the outer titanium layer (equivalent to 1.6 a.u. above the titanium surface in our way of calculation), led to the best agreement with the Eastman UPS experimental data.[72] Cremaschi and Whitten[73] also carried out SCF-CI calculations on chemisorption of hydrogen on titanium. Their conclusion was that dissociation of H_2 occurs above the surface but more stable 3-fold coordination sites lie closer to the surface at 1.3Å (2.46 a.u.).

In spite of the uncertainty in total energy of the Xα-SW method due to the muffin-tin approximation, we employed the method to do calculations on two different titanium-hydrogen systems, namely HTi_4 and Ti_4H. In the case of HTi_4, the hydrogen atom is at the underlayer tetrahedral hole. On the contrary, for the Ti_4H case the hydrogen atom is at the overlayer 3-fold hcp coordination site, 2 a.u. above the titanium surface. Figure IV-3(c) and Figure IV-3(d) show the density of states (DOS) for HTi_4 and Ti_4H respectively. Near the Fermi energy, the two different geometries behave in almost the same manner. However a large difference occurs on the left hand side far away from the Fermi energy. According to the DOS of HTi_4, the hydrogen induced peak is located at E=0.79 Rydbergs, which is 0.52 Rydbergs (7 eV) below E_F, while in the Ti_4H case, the position of the hydrogen induced peak is at E=0.61 Rydbergs which is 0.35 Rydbergs (4.8 eV) below the Fermi energy. Eastman's data suggested the

Figure IV-3 Density of states for (a) H, (b) Ti_4, (c) HTi_4, and (d) Ti_4H. The Fermi energies are indicated by a dashed line. The H induced states are illustrated in the diagrams by an arrow.

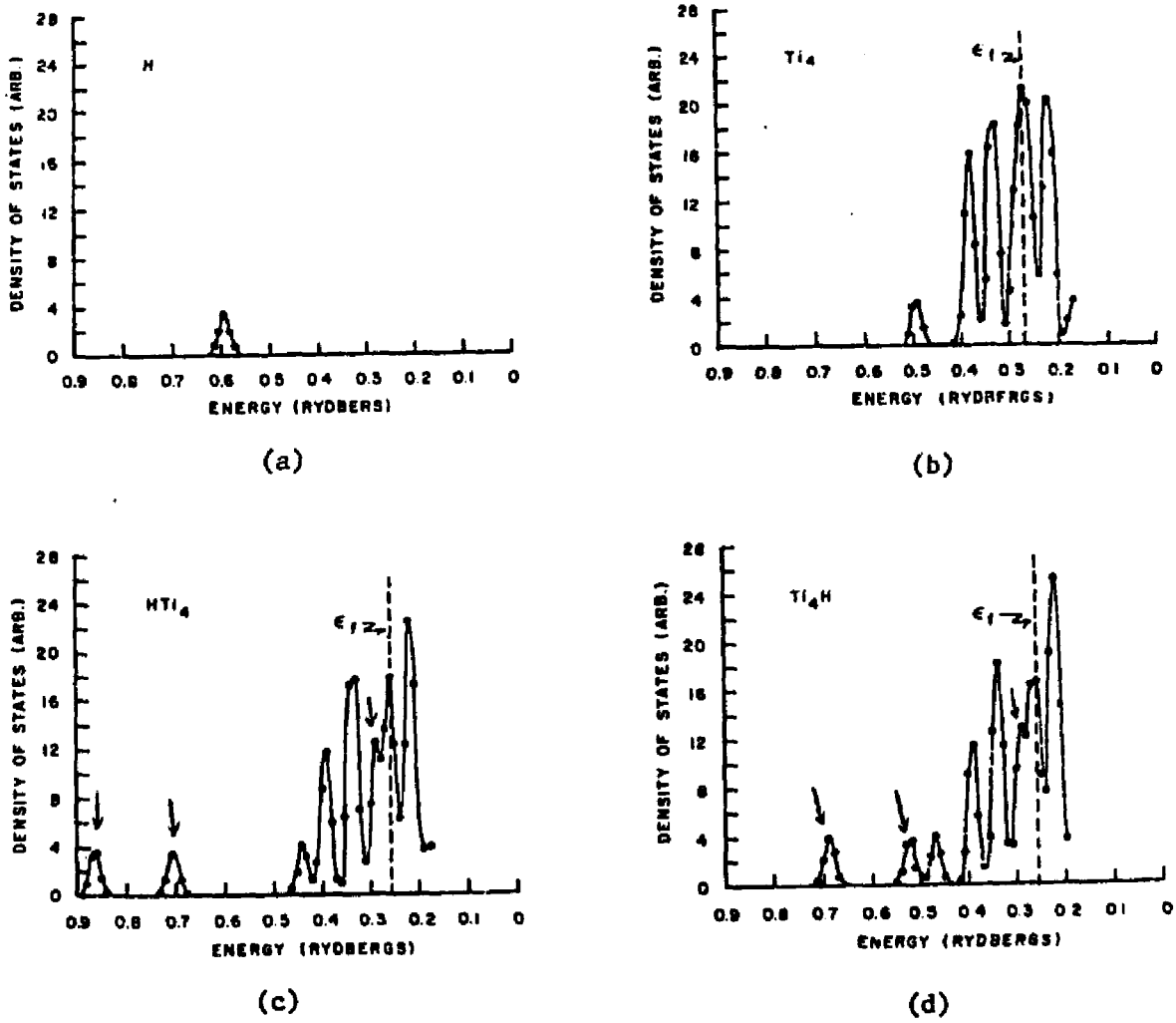

hydrogen peak should be at 5 eV below E_F as shown in Figure IV-4. Therefore, by identifying the position of the hydrogen peak, our calculation shows that for the Ti_4H case with a hydrogen atom siting on 3-fold hcp site, 2.0 a.u. above the Ti surface, the location of the peak agrees very well with experiment. On the contrary, the HTi_4 case shows that the position of the hydrogen induced peak is not in agreement with Eastman's experimental data.

IV-3-3 The Interaction of Atomic Hydrogen With Ni and Ti Clusters

The interaction of hydrogen with transition metals such as Ni and Ti is of fundamental importance in the understanding of the dissociative chemisorption of hydrogen on the surface of these metals[4] and the catalytic activity of small particles and clusters of these metals.[74] Both nickel and titanium belong to the first row of the transition metals in the periodic table. The primary difference between them is the fact that nickel is on the right hand side while titanium is on the left hand side of the transition metal group. Atomic nickel has the electron configuration of $(4\underline{s})^2(3\underline{d})^8$ while atomic titanium has the electron configuration $(4\underline{s})^2(3\underline{d})^2$. The relativistic effect on the first row of the transition metals is negligible. Molecular-orbital calculations were carried out for the titanium clusters using the standard nonrelativistic SCF-Xα-SW method. The Ti_4 and HTi_4 (hydrogen at tetrahedral hole) are open shell systems since each titanium atom has two unpaired $\underline{d}$ electrons. Therefore the

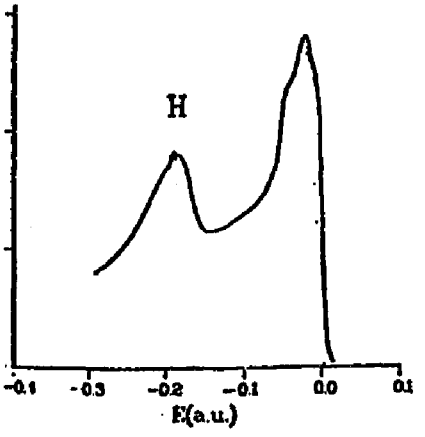

Figure IV- 4 Eastman's UPS spectrum for a Ti film. The energy zero in the curve is at the Fermi energy. 1 a.u. = 2 Rydbergs.

Figure taken from : D. E. Eastman, Solid State Commun. 10, 933 (1972).

unrestricted SCF-Xα-SW method was used for the calculation on the Ti_4 and HTi_4 systems. Only restricted SCF-Xα-SW results for Ni_4 and HNi_4 are available from Messmer's paper.

The resulting orbital energies for the tetrahedral cluster with and without interstitial atomic hydrogen are shown in Figure IV-5. Also shown, for comparison, is the SCF-Xα-SW 1s-orbital energy for the isolated hydrogen atom. The 1s-orbital energy of the hydrogen atom computed by the SCF-Xα-SW method corresponds approximately to to the electronegativity $\frac{1}{2}$ (I+A), where I is the ionization potential and A is the electron affinity.

The electronic structures of tetrahedral titanium and nickel clusters shown in Figure IV-5 are characterized by a manifold of closely spaced d-levels bracketed by s, p, d-hybrid levels. This is analogous to the overlap of the "d-band" by the "s, p - like conduction band" in the bulk Ti and Ni crystalline metals.[75] The Fermi level (E_F) passes through the top of the "d-band", just as in the bulk transition metals. The deepest energy level shown in Figure IV-5 for the Ti_4 cluster, associated with cluster orbitals having the a_1 representation of the T_d point group and roughly analogous to the Bloch band-structure state having the Γ_1 representation of the crystal space group, is predominantly s-like with a small amount of p, d-hybridization. The deepest energy level for the Ni_4 cluster, shown in Figure IV-5, is also associated with the a_1 molecular orbital, and is predominantly s-like, but with significant d-orbital hybridization and some p-like

Figure IV-5 SCF-Xα-SW orbital energies of tetrahedral nickel and titanium clusters with and without interstitial atomic hydrogen.

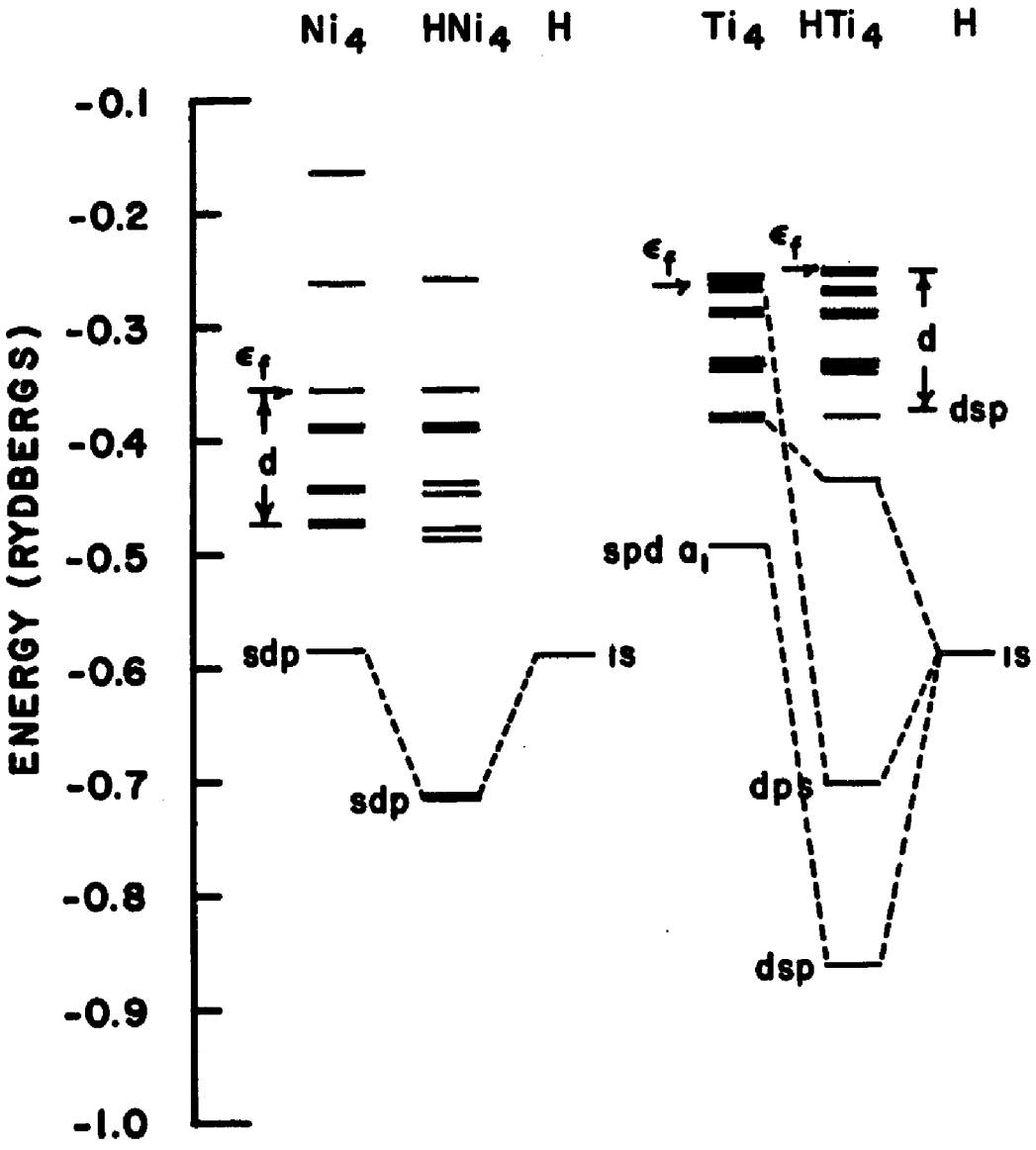

character. The partial-wave decomposition of the cluster orbitals having a_1 symmetry is summarized in Table IV-6. The main difference between Ni_4 and Ti_4 clusters is that Ni_4 has significant d orbital participation in the lowest σ bonding state, while Ti_4 has only a small amount. Ti_4 has a stronger s-like orbital in the lowest σ bond state. These differences between the electronic structure of Ti_4 and Ni_4 are important to understanding the differences in the photoemission spectra for hydrogen chemisorbed on these metals.[76] Those spectra indicated that hydrogen is always an impurity of a Ti film but not of a Ni film. We suppose that the difference of the lowest σ bond state between Ti and Ni is responsible for this difference due to the stronger Ti-H bond.

The covalent bonding of atomic hydrogen at the cluster interstitials is governed principally by the proximity in energy (or electro-negativity) and concomitant overlap of the symmetry-conserving a_1 orbitals near the bottom of the Ti_4 and Ni_4 d-bands with the H 1s-orbital. The main result is the splitting off of a hydrogen-metal bonding energy level of a_1 orbital symmetry from the bottom of the d-band of each cluster, accompanied by a small shift of the second lowest a_1 orbital, as indicated in Figure IV-5 by the orbital energies for the HNi_4 and HTi_4 clusters and the connecting dashed lines. The metallic 4s-like component of the lowest a_1 orbital is largely responsible for the bonding of hydrogen to the nickel aggregate, as indicated by the partial-wave decomposition for the a_1 orbital of lowest energy in Table IV-6. However, the contribution of the

Table IV-6 Partital-wave decomposition of the lowest a_1 molecular-orbital charge distribution of tetrahedral Ti and Ni clusters with and without interstitial atomic hydrogen.

Cluster	Orbital Energy (in Rydbergs)	Fraction Partial-Wave Character		
		s	p	d
Ti_4	0.494	0.79	0.11	0.09
HTi_4	0.864	0.31	0.28	0.41
Ni_4	0.580	0.63	0.11	0.26
HNi_4	0.724	0.47	0.18	0.35

3d-like component to the bonding is not negligible, amounting to 35% of the Ni_4-H a_1 bonding orbital charge. In contrast to the result for HNi_4, the metal d-orbital components almost dominate the bonding of hydrogen to the titanium aggregate, the contribution of Ti 4s-like components amounting to only 31% while the Ti 3d-like orbital component amounts to as high as 41%. This result underscores the danger of making general conclusions about the dominance of s-orbitals over d-orbitals in determining the chemisorption and catalytic reactivity of hydrogen on transition metals.

For both Ni_4 and Ti_4, the p-like orbital contributes only 11% of the a_1 bonding orbital which is not significant compared to the s-like orbital. The p-like orbital still is a minority participator of the Ni_4-H a_1 bonding since the 18% of the p contribution is about half of d-like orbital and one-third of s-like orbital. On the contrary, the p-like orbital shows its importance in the HTi_4 system, amounting up to 28% of the Ti_4-H a_1 bonding orbital charge which is about the same as the s-like orbital (31%). However, the p-orbital participation may be a function of cluster size.

One more important difference between HNi_4 and HTi_4 is the energy shifts upon H adsorption of the a_1 bonding state which are quite different. The energy shift of the a_1 orbital for Ti_4 and HTi_4 is 0.371 Rydbergs while the energy shift of the a_1 orbital for Ni_4 and HNi_4 is only 0.128 Rydbergs, one-third of the shift from a_1 of Ti_4 to a_1 of HTi_4. From this we can predict that the Ti_4-H a_1 bond is stronger

than the Ni_4-H bond. The interaction between hydrogen and Ti_4 cluster is a stronger interaction than the interaction between hydrogen and Ni_4 cluster. This may explain why all the photoemission data of Ti film show a hydrogen induced peak, which is not seen on the Ni film.

CHAPTER V

CORRELATED WAVE FUNCTION CALCULATION OF THE CHEMISORPTION OF NITROGEN ON Ti(0001)

V-1 Introduction

The chemisorption of N_2 on transition metal surfaces has been the subject of many experimental studies.[38,77-81] Most structures of chemisorbed species on metal surfaces involve overlayer formation on the surface, i.e., with the adatoms located above the outermost layer of the metal surface. However, there has been both theoretical and experimental evidence for underlayer formation when nitrogen is chemisorbed on titanium.[38,80-82] The chemisorbed structure of nitrogen on Ti(0001) is apparently a structure for which the atomic arrangement reflects very closely the structure of the bulk compound TiN, the N atoms being located underneath the top layer of Ti atoms in what are usually called octahedral interstitial positions.

Shih et al[38,81] have done LEED experiments and theoretical LEED intensity calculations based on the layer Korringa-Kohn-Rostaker method to determine the surface structure of nitrogen on Ti(0001). Figure V-1 shows their LEED data and calculated spectra. Upon the LEED analysis of the 1 × 1 structure, they conclude that the N atoms are located in the octahedral holes 1.22 ± 0.05Å below the first layer of Ti atoms. The description of the octahedral hole geometry is shown in Figure V-2. Each N has six nearest neighbors. This unique result among all experiments-underlayer formation - provides motivation for the calculation of chemisorption of N_2 on Ti.

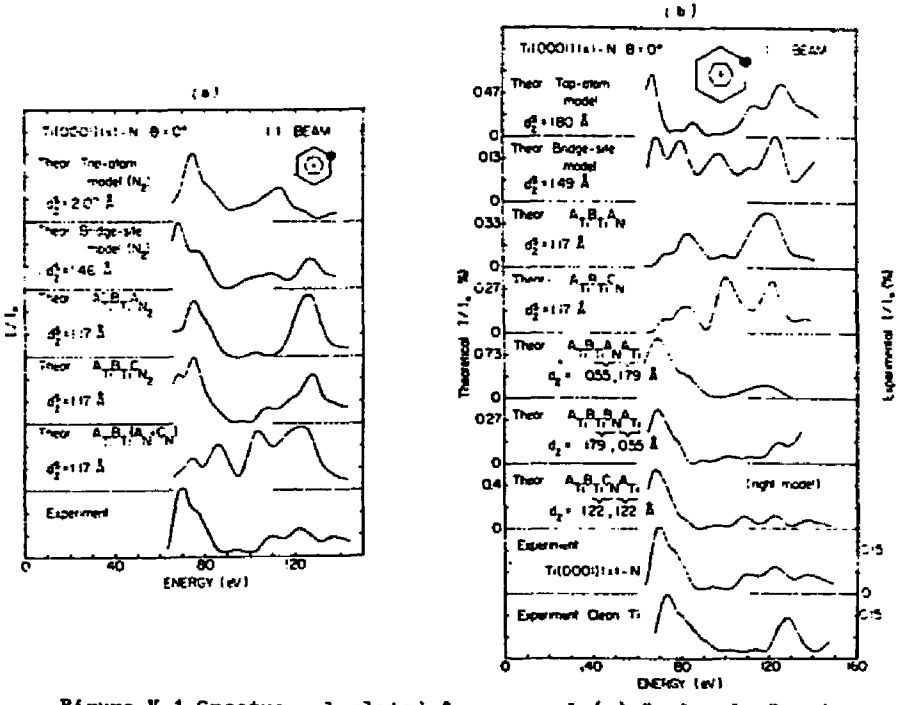

Figure V-1 Spectra calculated for several (a) "molecular" and (b) "atomic" models are compared with LEED data.

Figures taken from: H. D. Shih, F. Jona, D. W. Jepson and P. M. Marcus, Surf. Science 60, 445(1976).

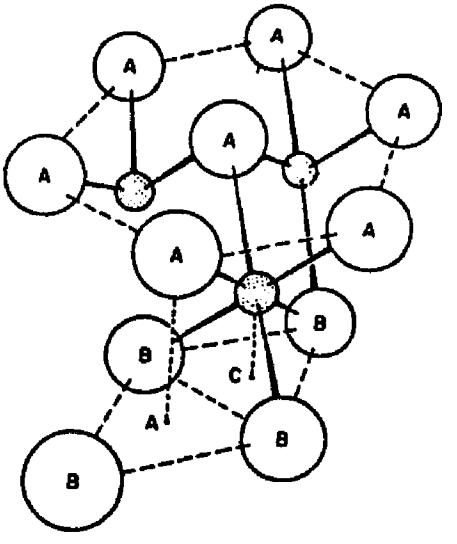

FIG. V-2 Perspective view of the Ti(0001)1×1-N structure. The circles marked *A* represent close-packed Ti atoms in the top atomic plane; the circles marked *B*, close-packed Ti atoms in the second plane. The smaller dotted circles represent N atoms sandwiched between the two Ti planes. Only for the nearest N atom is the full octahedral coordination indicated by bond lines. The dotted vertical lines indicate the registry of the *A* Ti atoms and of the N atoms relative to the close-packed *B* plane.

Figure taken from: H. D. Shih, F. Jona, D. W. Jepsen and D. M. Marcus, Phys. Rev. Lett. 36, 798 (1976).

In this work we consider the theoretical treatment of the adsorption and dissociation of a single N_2 molecule on a Ti(0001) surface using an electronic theory that permits the accurate computation of molecule-solid surface interactions. The SCF-CI theory is based on a many-electron approach in which configuration interaction follows ab initio SCF calculations on an adsorbate plus surface region embedded in the remainder of the lattice. The following objectives are set:

(a) Calculation using small clusters, N_2-Ti_{10}, to determine preliminary information about the potential surface for N_2 on Ti(0001), involving the approach to the surface, atop atom, bridge, semi-octahedral and 3-fold octahedral adsorption sites.

(b) Calculation of selected N_2 adsorption sites, including the octahedral interstitial position, using the embedding scheme[73] for a more realistic 26 atom, three layer cluster model of the Ti(0001) surface.

(c) The delineation of contributions of 4s and 3d electrons to bonding and the importance of correlation effects on adsorption, and

(d) the comparison of adsorption results for large and small Ti clusters.

V-2 Free N_2 Molecule Calculation

The free nitrogen molecule calculation was needed for three reasons. The first reason is to verify the validity of the nitrogen basis set which we adopted.[83] The second is to determine the internuclear distance which gives the maximum bonding energy between the two nitrogen atoms for this nitrogen basis set. This distance shall be treated as the unstretched equilibrium bond distance of the free nitrogen and shall be used for the unstretched case of the titanium-nitrogen chemisorbed calculations. The third is to find the total energy of the free nitrogen molecule with the unstretched equilibrium bond distance. This energy plus the total energy of a chosen lattice shall be used as a reference for calculating the binding energies of the chemisorbed system.

The nitrogen molecule is the adsorbate which is chosen for the underlayer formation chemisorption studies in accordance with the LEED data. The atomic cores of the nitrogen atoms in the N_2 molecule are not assumed to be frozen. All electrons in the N_2 molecule are involved in the entire SCF calculation. The N_2 basis was chosen as 1s, 1s', 2s, 2s', 2px, 2p'x, 2py, 2p'y, 2pz and 2p'z on each nitrogen atom. The parameters were taken from Whitten's paper.[83] The results of the SCF-CI calculation on the free N_2 molecule are tabulated in Table V-1. At the SCF level, the energy minimum occurs at the bond distance of 2.09 a.u.. However, with the consideration of configuration-interaction, the new energy minimum is shifted to the

Table V-1 Results of the SCF-CI Calculation on the N_2 Molecule.

R_{N-N} (a.u.)	E_{SCF} (a.u.)	C.I. (a.u.) Lowering	E_{SCF+CI} (a.u.)
1.99	-108.8631	-0.1837	-109.0468
2.04	-108.8694	-0.1887	-109.0581
2.09	-108.8706	-0.1927	-109.0633
2.14	-108.8675	-0.1981	-109.0656
2.19	-108.8609	-0.2028	-109.0637
2.24	-108.8534	-0.2080	-109.0614
3.2	-108.4976	-0.3050	-108.8026

where

R_{N-N} - bonding distance between two nitrogen atoms.

E_{SCF} - total energy of N_2 at SCF level only.

C.I. - configuration interaction.

$E_{SCF + CI}$ - total energy of N_2 including SCF & CI calculation.

bond distance of 2.14 a.u.. These results are in good agreement with the experimental value, 2.074 a.u..[84] The total energy of a nitrogen atom is 54.3881 a.u..[83] Taking this number as a reference, we found the binding energy of a nitrogen molecule at the bond distance 2.14 a.u. is 7.87 eV. The experimental binding energy of the N_2 molecule is 9.91 eV.[84] Therefore our calculated free N_2 binding energy is less than the experimental data by 2.04 eV. However, this result is an improvement compared to the calculated value of the restricted Hartree-Fock method, 5.27 eV.[84]

V-3 Small Cluster Calculation, $Ti_{10}N_2$

The simplest possible model of the Ti(0001) surface with at least two semi-octahedral adsorption sites is a two layer structure of ten atoms, defined by the seven atoms with a close-packed hexagonal structure as the top layer and the three atoms of the second layer located at every other three fold site underneath the top layer. Figure V-3 shows the two layer structure of Ti_{10}. In this section, N_2 adsorption on such a Ti_{10} cluster is treated at an elementary level to obtain preliminary information about the potential surface and preferred adsorption sites. Due to the small size of the cluster, no exterior region is defined by localization, and all Ti atoms have the same set of basis orbitals, 4s and 4s'; the N_2 basis consist of 1s, 1s', 2s, 2s', 2px, 2p'x, 2py, 2p'y, 2pz and 2p'z orbitals. The 3d electrons of the metal, as a first approximation, are assigned to atomic cores and contribute only an electrostatic potential. Calculations generally are performed only at the SCF level, but for some key points on the surface CI calculations are carried out to examine relative stabilities. Binding energies are reported in Table V-2 and Table V-3 for numerous points on the potential surface involving four sets of perpendicular approaches of N_2 to the Ti surface and six sets of parallel approaches respectively. In all cases, binding energies are given by taking the energy of the Ti_{10} clean surface plus that of the free N_2 molecule as a reference.

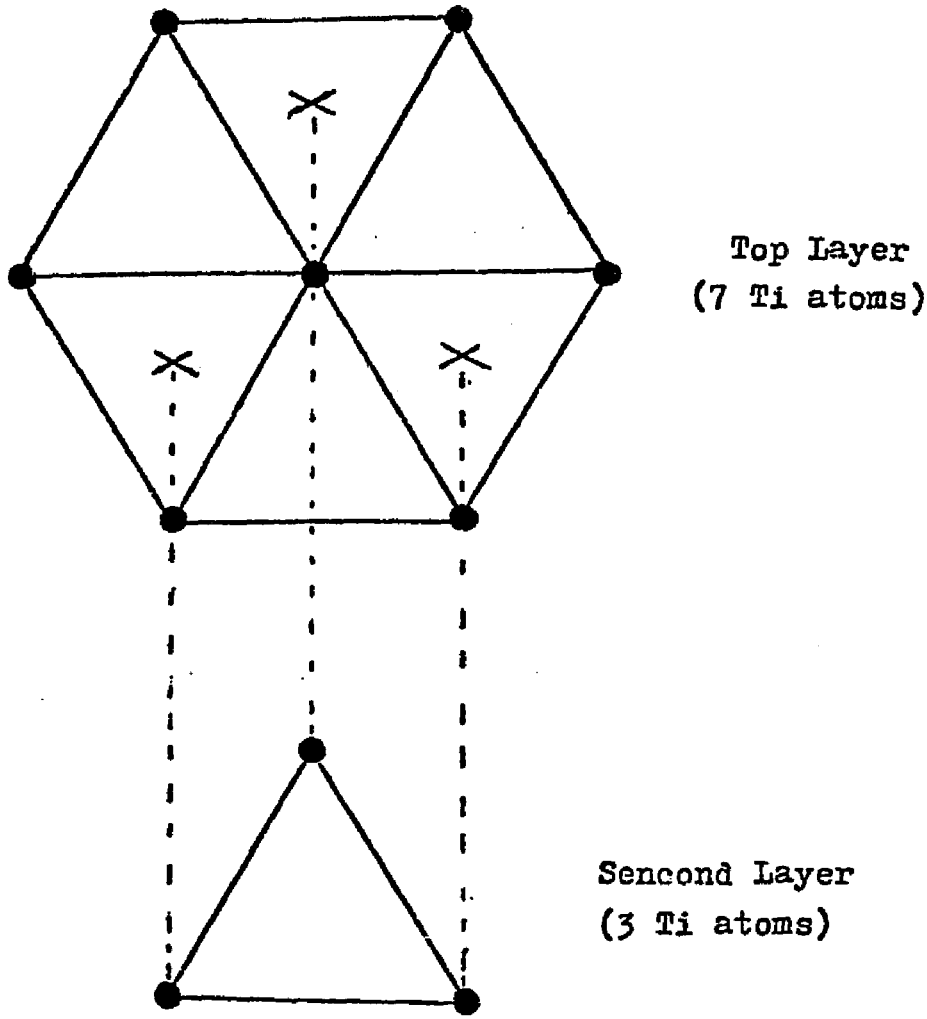

Figure V-3 Structure of Two Layer Ti_{10} Small Cluster Model

Case	Geometry	$N_{(1)}$-$N_{(2)}$ Distance (a.u.)	Distance above surface (a.u.) & Binding energies(ev)					
			R=5.0	4.5	4.0	3.5	3.0	2.5
A		2.14	-0.71			-0.31	-0.47	-1.01
		2.45				-0.57		
B		2.14				-0.16	-0.21	
C		2.14				-1.76	-3.67	
D		$N_{(1)}$ above the surface $N_{(2)}$ at a semi-octahed. site		-3.75	-3.80	-4.00		

Table V-2 Adsorption sites for N_2 on Ti_{10} and binding energies of four sets of perpendicular approaches. A negative binding energy indicates a repulsive state.

Case	Geometry	$N_{(1)}$-$N_{(2)}$ Distance (a.u.)	Distance above surface (a.u.) & Binding energies(ev)					
			R=5.0	4.5	4.0	3.5	3.0	2.5
E		2.14			-0.94	-0.85	-1.52	
F		3.22					-2.10	
G		6.44					-6.14	
H		5.58					-3.54	
I		5.58					-6.96	
J		5.58	$N_{(1)}$ and $N_{(2)}$ are located at two adjacent semi-octahedral sites. The binding energy is -1.37 ev.					

Table V-3 Adsorption sites for N_2 on Ti_{10} and binding energies of six sets of parallel approaches. A negative binding energy indicates a repulsive state.

In Case A of Table V-2, at an $N_{(1)}$ distance of 3.5 a.u. (1.85 Å) above the surface of the three-fold hcp adsorption site, an energy minimum occurs for a N - N bond that is unstretched from the free molecule value of 2.14 a.u.. The only stretched case considered, for a distance 2.45 a.u. between two nitrogen atoms, 0.3 a.u. more than the free molecule value, turned out to be energetically unfavorable. In Case B of Table V-2, at an $N_{(1)}$ distance of 3.5 a.u. above the surface of the three-fold fcc adsorption site, the lowest energy is obtained of all the cases considered and has binding energy -0.16ev.

Contrary to one of the results in the calculation of H_2 on Ti_7,[73] the perpendicular approach of N_2 directly above the central atom is the most unstable. Another interesting result occurs for the perpendicular approach Case D of Table V-2, where the second atom ($N_{(2)}$) is fixed at the semi-octahedral site and the first atom ($N_{(1)}$) remains on the surface of the fcc adsorption site. The binding energies are unfavorable for the $N_{(1)}$ atom moving closer to the lattice. This suggests that once one of the two atoms in a nitrogen molecule overcomes the activation barrier to find a favorable location at the octahedral site, a second N atom can no longer have a suitable site nearby on the surface of the lattice.

All six sets of parallel approaches are energetically unfavorable as shown in Table V-3. However, the results do suggest that molecular adsorption is less unfavorable energetically than dissociative adsorption. A local energy minimum of Case E appears again at 3.5 a.u. above the lattice surface. The bridge and 3-fold coordination sites

are less stable. The most unstable position is found at the fcc-fcc 3-fold coordination sites.

Case J of Table V-3 is special since the two nitrogen atoms of a nitrogen molecule are both located inside the surface. The two nitrogen atoms of a nitrogen molecule are separated and are located at the two adjacent semi-octahedral adsorption sites between the first (top) layer and second layer of the Ti_{10} cluster model. A semi-octahedral site is a site which is missing one atom compared to an octahedral site. Cases H, I and J have a common $N_{(1)} - N_{(2)}$ distance of 5.7 a.u.. Among these three different cases, Case J which is the only underlayer calculation shows a relatively favorable energy.

From the discussion above, the Ti_{10} small cluster calculations give us some important information. First of all, the unstretched perpendicular adsorption at 3.5 a.u. above the surface is the most energetically favorable case among all the cases investigated. Secondly, no bonding is produced at the SCF-CI level of calculation for overlayer formation. This is a surprise because small clusters tend to overemphasize bonding due to the unrealistically large number of surface atoms present. This could mean that the d electrons will play an important role. Perhaps they have to be singly occupied in this SCF-CI calculation, as is suggested by results of Melius,[31] Pakkanen[50] and our $X\alpha$-SW-SCF calculation. These previous calculations

have shown that singly occupying the d's gives lower energies. Thirdly, an underlayer formation geometry, consisting of two nitrogen atoms at two adjacent octahedral adsorption sites is relatively favorable in these small cluster calculations.

V-4 Large Cluster Model, $Ti_{26}N_2$

The Ti(0001) surface was modeled by a 26 Ti cluster for N_2 adsorption studies. The cluster, shown in Figure V-4, consists of three layers: the surface layer of 16 atoms, a second layer of 5 atoms, and a third layer of 5 atoms. This cluster is part of the 54 atom lattice in Ref. 15 with internuclear distances the same as in bulk Ti. A ten atom subregion (five of surface layer plus five of second layer) including overlayer hcp, fcc and underlayer octahedral adsorption sites was specified for the N_2 adsorption studies. The orbital basis for these atoms was augmented by one additional $4\underline{s}$ and one $3\underline{d}$ basis function. A double zeta basis was used for N_2 and the single zeta basis of Ref. 15 was employed on the remaining lattice atoms. The core potentials are derived from the spherically averaged Ti atom configuration $(4\underline{s})^1\ (3\underline{d})^3$. A unitary localization transformation was carried out following the SCF procedure using all 12 nitrogen 2p orbitals and the neighboring Ti atoms of the adsorption region to define the localization site. This procedure limits the CI to a tractable subspace of localized electrons and at the same time incorporates the delocalized character of the $4\underline{s}$ band into the local description.

All calculations are performed as follows. The Ti $3\underline{d}$ electrons are localized in a $\underline{d}^3$ atomic distribution on all Ti atoms except the ten atoms bordering the N_2 adsorption sites. On these atoms a spherically averaged $\underline{d}^2$ distribution is defined by an effective

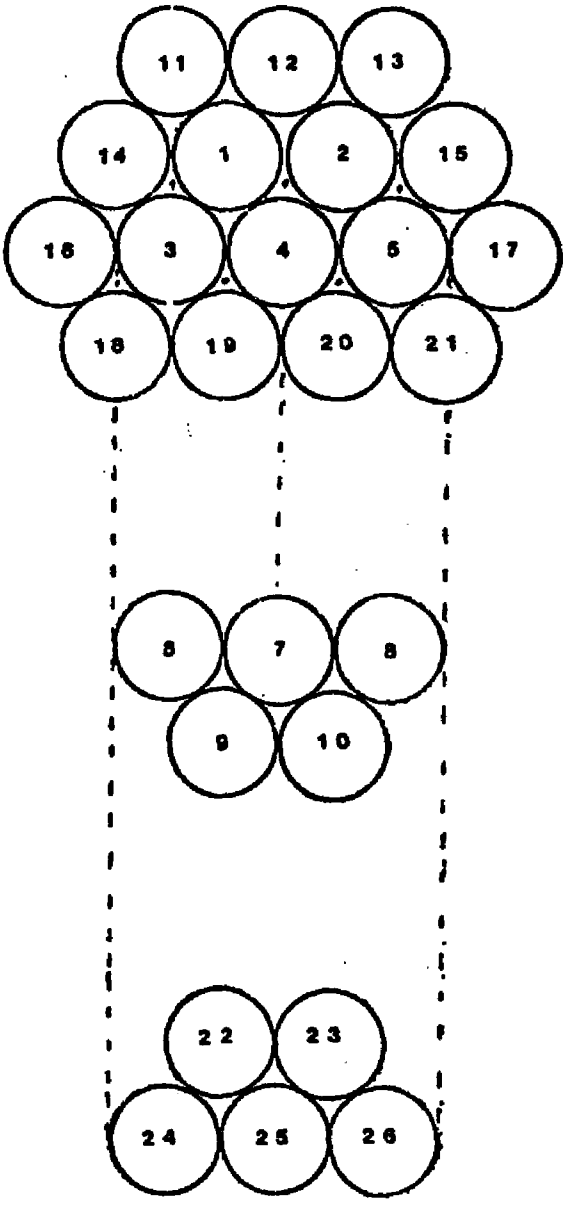

Figure V-4 Titanium hcp cluster containing 26 atoms. The localization site in the surface and second layer is labeled by atoms 1-10.

potential including a d/valence orbital overlap projector; the remaining d electron basis orbital is treated explicitly by allowing mixing with the s, p electrons in either singly or doubly occupied orbitals in the SCF description. An open-shell procedure was needed in this SCF calculation due to the absence of bonding in the small cluster ($Ti_{10}N_2$) calculation and also because of evidence the energy is lowered by singly occupying the d orbitals in the previous $X\alpha$-SW calculations. Following the SCF calculation the splitting of Ti-3d levels in the resulting field is determined, and the energy lowering due to the transfer of two spherically averaged d electrons to the two lowest d levels per Ti atom is calculated by taking the difference between the energy total of the two lowest levels and twice the value of the averaged energy of the four lowest lying levels of a Ti atom. This energy lowering is added to the SCF energy, and likewise indirectly to the final total energy which includes the CI contribution. The purpose of the CI is two fold: to introduce electronic correlation in the description of adsorbate-surface bonding and to permit further variation in the coupling of the d electrons in the local bonding region.

Preliminary calculations on Ti_{10}-N_2 (2-layer) showed the energetically most favorable case to be: N_2 unstretched and perpendicular to the surface at the three fold fcc coordination site at 1.85 Å (3.5 a.u.). The Ti_{10}-N_2 small cluster calculation also suggested another favorable site with underlayer formation with the two nitrogen atoms at two adjacent octahedral adsorption sites.

Based on this information, three geometries were considered and listed below for N_2 above the Ti_{26} surface and N_2 at the underlayer octahedral sites

A. N_2 and Ti_{26} at infinite separation.

B. N_2 axis perpendicular to surface with nearest N 3.5 a.u. (1.85 Å) above surface at fcc 3-fold coordination site.

C. Two N atoms in neighboring octahedral holes.

Figure V-5 shows the SCF eigenvalues for N_2 on Ti(0001). For the N_2 and Ti_{26} separated case, the Ti lattice levels (between -0.10 a.u. and -0.34 a.u.) are well separated from the N_2 levels (between -0.60 a.u. and -1.55 a.u.). There is also a fairly narrow "d" band of lattice orbitals. Perpendicular adsorption results show a slight downshift (~1 eV) of the N_2 σ and π levels when compared to the free N_2 case. Also the d band is somewhat broadened. This spectrum corresponds qualitatively to that of free N_2. For the underlayer adsorption case, the eigenvalue spectrum changes significantly. The major feature of the underlayer formation is the sharp upward shift in all levels. This is due to the fact that each N atom has taken up about 1.6 extra units of electronic charge compared to free N_2. While comparison with the photoemission data[80] are difficult due to several complications (described below), the underlayer formation case 2s and 2p levels lie much closer to the photoemission 2s and 2p levels than do those for the perpendicular adsorption case.

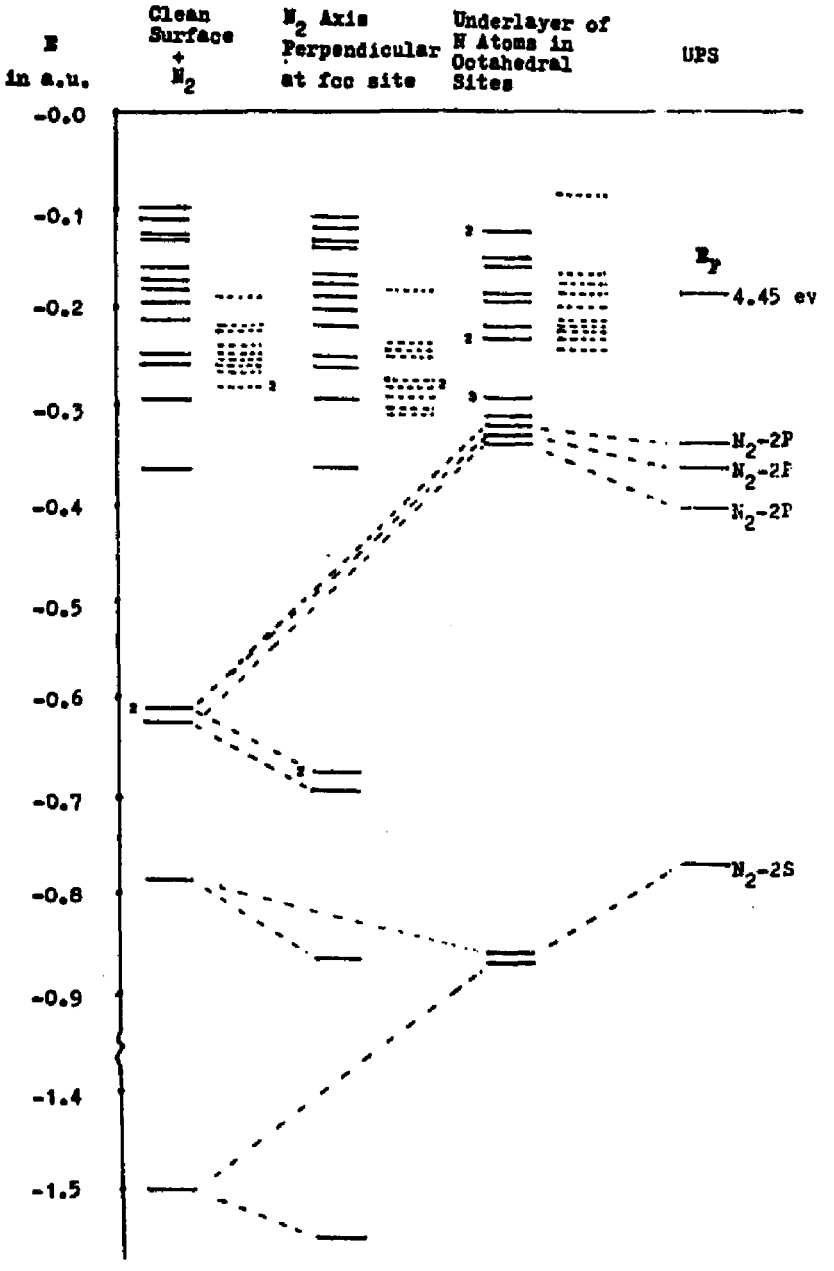

Figure V-5 SCF eigenvalues for N_2 on Ti(0001). Solid lines represent the doubly occupied states. Dashed lines denote the pure Ti 3d singly occupied levels.

* UPS data were taken from : P. J. Feibelman and F. J. Himpsel Phys. Rev. B 21, 1394(1980).

Complications referred to above:

(1) - We are calculating the very dilute case whereas the UPS experiment deals with monolayer coverage. Thus nitrogen-nitrogen interactions could affect the results. These interactions are not included in our calculation.

(2) - Electronic relaxation effects are not properly included by using Koopman's theorem to obtain the ionization energy. Work is in progress to include relaxation effects by doing SCF calculations.

(3) - Inadequate treatment of screening effects of the N-2s electrons. The screening effects could be important in a calculation of the ionization potential of this core-like level.

In Table V-4, total SCF energies and correction terms due to the superposion effect of the basis set are reported for each adsorption site. Calculated binding (adsorption) energies relative to the N_2 molecules and Ti_{26} clean surface are given in Table V-5. Of the sites investigated, the underlayer formation with two nitrogen atoms separately at the two adjacent octahedral adsorption sites is the most stable with a large binding energy, 0.183 a.u. (115 kcal/mole). The overlayer perpendicular case is not bound. There are thermochemical data for comparison. King and Tompkins[78] observe a weakly bound state for N on Ti with binding energies between 6 and 20 kcal/mole with monolayer coverage. Fromm and Mayer[79] observe a strongly bound state (~80 kcal/mole) with about two nitrogen layers of coverage. These data are in qualitative agreement with our calculated binding

Table V-4 Total SCF energies and the correction energies of the superposion effect for N_2-Ti_{26} adsorption cases.

Site	Total E_{SCF}	Correction for superposition effect	Total energy after correction
N_2 - Ti_{26} separated	-116.657	0.0	-116.657
N_2 axis perpendicular at fcc site	-116.619	+0.020	-116.599
Two N atoms in adjacent octahedral holes	-116.922	+0.138	-116.784

Table V-5 N_2 adsorption on Ti(0001). Calculated binding energies for N_2 adsorption at selected sites are reported for successive refinement in theoretical treatment. Energies in a.u.

Site	E_{scf} Including Superposition of Basis Sets Effect	Correction For d Electron Level Splitting in Field of Adsorbate	CI Lowering	Binding ΔE
N_2 - Ti_{26} Separated	0.0	0.0	0.198	0
N_2 Axis Perpendicular to surface at fcc Site	-0.058	0.004	0.157	-0.095
Two N atoms in adjacent Octahedral Holes	+0.127	0.112	0.142	0.183* (115 Kcal/Mole)

* D. A. King and P. C. Tompkins -Weakly Bound State, 6-20 Kcal/mole, Trans. Far. Soc. 64, 496 (1968).
E. Fromm and C. Mayer - Strongly Bound State, 80 Kcal/mole, Surface. Sci. 57, 775 (1976).

energies which show a strongly bound underlayer geometry and a nearly bound state for a typical overlayer geometry.

A complete calculation of binding energies for all the cases involves several extra steps. The details are described below:

(1) Superposition of basis set effect.

This calculation is the correction due to superposition of basis set effect. One would expect this effect to be especially large when the nitrogen basis is actually inside the lattice. The error arises because the lattice actually "borrows" some of the nitrogen basis and lowers the energy at the combined system. Thus it is not correct to calculate the binding energy with respect to the lattice unless some correction is taken for this effect. Thus, the energy of the lattice is calculated using the full nitrogen basis in addition to the Ti basis. This may overestimate the effect slightly since the nitrogen orbitals are occupied by electrons contributed by the nitrogen. However, since the superposition difficulty arises due to the diffuse part of the orbitals, it is better to assume the full effect than to ignore it. This correction for the overlayer perpendicular case is not significant with a small correction 0.020 a.u. compared to 0.138 a.u. of the underlayer formation case.

(2) $\underline{d}$ electron splitting effect

Initially we assumed the electronic configuration for a titanium atom in the lattice is $(3\underline{d})^3\ (4\underline{s})^1$. This configuration is a reasonable one based on our SCF-Xα-SW and other workers' results.[31,50] Of the

three 3d electrons per atom, one was explicitly included in the SCF calculation while the other two were represented by a spherically symmetric core potential obtained from a spherically symmetric charge distribution representing the remaining "d" electrons.

Since the d electrons are well localized it is reasonable to study their behavior in the fixed field of the nuclei and electrons of the lattice and adsorbate given by the SCF calculations. The 5 d electron levels for each of the ten "improved" Ti atoms are shown in the Table V-6 for the clean surface, underlayer, and overlayer perpendicular adsorption cases. These levels were obtained by diagonalizing the energy matrix for the 5 d levels for each atom.

Analysis of the results showed that in each case the lowest energy levels obtained were those for which the d functions pointed away from the adsorbate atoms. Both overlap and Coulomb effects contributed to raising the energy levels when a d function pointed toward the adsorbate.

The amount of the lowering was estimated by calculating the energy difference between the states with the two lowest levels occupied and the case with the two electron energies averaged over the four lowest lying levels on each atom. Only the one-center part of the total energy was considered since there is virtually no overlap between the d functions on neighboring atoms.

In each case the d electron which was explicitly included in the SCF calculation had a higher energy than the highest lying d level on the same atom. Apparently a d level is pushed up by the rest of the electrons.

Table V-6 Five d electron levels for each of the ten "improved" Ti atoms for the three selected adsorption cases. Energies in a.u.

Case	Atom 1	Atom 2	Atom 3	Atom 4	Atom 5	Atom 6	Atom 7	Atom 8	Atom 9	Atom 10
Clean	-0.318	-0.313	-0.301	-0.334	-0.301	-0.314	-0.350	-0.313	-0.303	-0.306
Surface	-0.311	-0.306	-0.295	-0.328	-0.295	-0.306	-0.343	-0.306	-0.297	-0.301
+	-0.303	-0.298	-0.287	-0.321	-0.287	-0.304	-0.337	-0.304	-0.292	-0.295
N_2	-0.279	-0.273	-0.265	-0.299	-0.264	-0.280	-0.314	-0.280	-0.270	-0.274
	-0.245	-0.238	-0.230	-0.262	-0.229	-0.247	-0.272	-0.246	-0.228	-0.232
N_2 Axis	-0.322	-0.322	-0.307	-0.354	-0.309	-0.308	-0.355	-0.322	-0.314	-0.319
Perpendi.	-0.316	-0.317	-0.302	-0.349	-0.305	-0.300	-0.348	-0.314	-0.308	-0.314
at fcc	-0.307	-0.307	-0.293	-0.341	-0.294	-0.298	-0.342	-0.312	-0.303	-0.308
Site	-0.283	-0.283	-0.271	-0.319	-0.272	-0.273	-0.319	-0.288	-0.282	-0.287
	-0.250	-0.232	-0.237	-0.264	-0.222	-0.236	-0.272	-0.253	-0.242	-0.246
Underlay.	-0.259	-0.269	-0.260	-0.394	-0.260	-0.185	-0.142	-0.190	-0.189	-0.193
of N	-0.255	-0.265	-0.256	-0.391	-0.256	-0.180	-0.141	-0.186	-0.187	-0.192
Atoms in	-0.240	-0.250	-0.241	-0.383	-0.241	-0.162	-0.117	-0.169	-0.164	-0.169
Octahedr.	-0.216	-0.227	-0.218	-0.370	-0.217	-0.124	-0.107	-0.131	-0.130	-0.135
Sites	-0.150	-0.160	-0.150	-0.309	-0.149	-0.094	-0.080	-0.099	-0.099	-0.104

Note: The atoms are numbered in the same way as in Figure V-4.

(3) Correlation effects.

Finally CI calculations were carried out for the various geometries. Negligible effects due to d excitation were observed. One surprise was that the CI lowering for the perpendicular case, 0.157 a.u., is substantially less than for free N_2. This is surprising because N_2 in this case seems to be little altered from free N_2 which has a CI lowering of 0.198 a.u.. However there is some difference as is indicated by the fact that the charge on the nitrogen atom nearest the surface is 7.2 electronic charge while 6.8 units of electronic charge are on the more distant atom.

Another interesting calculated result indicating the formation of a bound state in the octahedral case is discussed as follows. In the process of reviewing the molecular orbitals for the underlayer octahedral case, we found an s-d mixing singly occupied orbital with some charge leakage from Ti-3d to Ti-4s . This may explain why the underlayer octahedral case forms a bound state while the other cases do not. The unique s-d mixing orbital is significant because the extra interaction between the Ti-3d and Ti-4s may lower the total energy of the system due to a gain in energy on delocalization.

V-5 Comparison Between the Calculations for the Overlayer Dissociated Case and the Underlayer Octahedral Case.

The large cluster ($Ti_{26}N_2$) calculations in Section V-4 indicated that the underlayer octahedral case shows a bound state with a binding energy of 115 kcal/mole. The eigenvalue spectrum for the underlayer octahedral case also shows good agreement with Feibelman's UPS data. However, we felt that the overlayer dissociated case may yield results similar to those of the underlayer octahedral case since the two nitrogen atoms in the overlayer case are exactly over their postulated underlayer positions. In spite of an unfavorable result for the dissociated case obtained from the small cluster calculations (section V-3), we did further calculations of the large cluster model for the overlayer dissociated case. The two nitrogen atoms of the overlayer dissociated case located at the two adjacent fcc sites are 3.5 a.u. above the Ti surface.

The calculated SCF eigenvalues for N_2-Ti_{26} systems, including the overlayer dissociated case, are shown in Figure V-6. The eigenvalue spectra of the doubly occupied orbitals for both the overlayer dissociated case and the underlayer octahedral case are similar. This is expected since the doubly occupied orbitals are mostly nitrogen orbitals with some titanium orbitals. The 2s and 2p levels of the nitrogen groups for the overlayer dissociated case have about the same value as those for the underlayer octahedral case. Thus, the eigenvalue spectrum for the overlayer dissociated

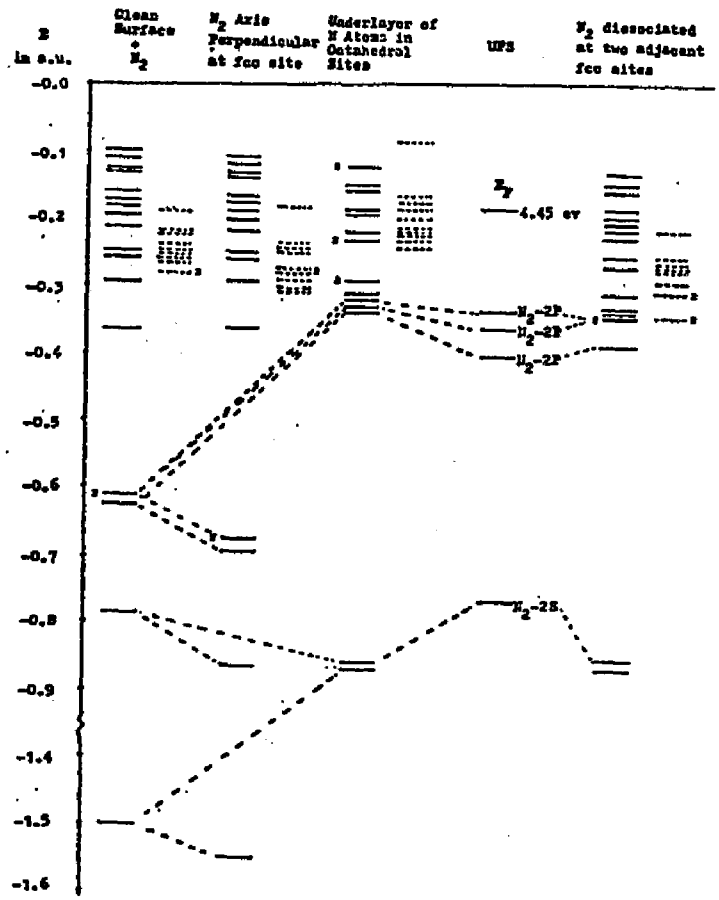

Figure V-6 SCF eigenvalues for N_2 on Ti(0001). Solid lines represent the doubly occupied states. Dashed lines denote the pure Ti 3d singly occupied levels. The calculated SCF eigenvalues for the overlayer dissociated case are also presented in this figure.

* UPS data were taken from : P. J. Feibelman and F. J. Himpsel Phys. Rev. B21, 1394 (1980).

case also agrees well with Feibelman's UPS data.[80] This indicates that using the eigenvalue spectrum alone to determine the correct binding geometry is not reliable. This argument is often used in connection with Xα-SW and band structure calculations on chemisorption. In order to make a correct judgement, we also have to take the total energy of the the system into consideration. The pure Ti singly occupied orbitals, however, show some differences between the overlayer dissociated and underlayer octahedral cases. Compared to the clean Ti surface case (see Figure V-6), the singly occupied orbitals for the overlayer dissociated case are downward shifted while the singly occupied orbitals for the underlayer octahedral case are upward shifted. The difference between the binding energies for these two cases is also shown in Table V-7. We found that the binding energy is negative (i.e. not bound) for the overlayer dissociated case. Besides, the negative binding energy is unusually high for the dissociated case. The high negative binding energy at the SCF level hints the existence of an intrinsic calculation problem in the calculation of the dissociated case. The first thought was that the spin problem may be at fault, since the dissociated nitrogen groups may prefer to have more singly occupied orbitals for their electrons. The results of the calculations are tabulated in Table V-8. We see that the changes are insignificant. Therefore, some other explanation must be sought in this calculation.

Table V-7 N_2 adsorption on Ti(0001). Calculated binding energies for N_2 adsorption at selected sites are reported for successive refinement in theoretical treatment. Energies in a.u.

Site	E_{scf} Including Superposition of Basis Sets Effect	Correction For d Electron Level Splitting in Field of Adsorbate	CI Lowering	Binding ΔE
N_2 - Ti_{26} Separated	0.0	0.0	0.198	0
N_2 Axis Perpendicular to surface at *fcc* Site	-0.058	0.004	0.157	-0.095
Two N atoms in adjacent Octahedral Holes	+0.127	0.112	0.142	0.183* (115 Kcal/Mole)
N_2 Dissociated at two adjacent fcc sites	-0.208	0.027	0.096	-0.283

* D. A. King and F. C. Tompkins -Weakly Bound State, 6-20 Kcal/mole, Trans. Far. Soc. 64, 496 (1968).
E. Fromm and O. Mayer - Strongly Bound State, 80 Kcal/mole, Surface. Sci. 57, 775 (1976).

Table V-8 The total energies for different numbers of singly occupied orbitals.

number of singly occupied orbitals	10	12	14	16
total energy in a.u.	-116.491	-116.512	-116.499	-116.507

Through analyzing the charge population, we found that each nitrogen takes about 0.7 electronic charge from the Ti lattice. This information led us to guess that the dissociated case needs an ionic calculation which includes more diffuse nitrogen basis functions. Thus, we carried out another calculation with more basis functions for the two nitrogen atoms. The new calculation used a triple zeta basis function instead of a double zeta basis function for each of the $2\underline{s}$, $2\underline{p}_x$, $2\underline{p}_y$, $2\underline{p}_z$ orbitals for the two nitrogen atoms. The old calculation used 66 basis functions while the new calculation employed 74 basis functions for the entire system. The comparisons between the results of the new and old calculations are listed in Table V-9. The data show that the total energy of the new calculation is lower than that of the old calculation by 0.022 a.u.. However, two pieces of evidence indicate that this change is too small to be significant. The first piece of evidence is that the negative binding energy is still too high to form a bound state. The second piece of evidence is that the charge populations for the basis functions of the new calculation are about the same as those of the old calculation. The charge populations in the eight new basis functions of the new calculation are near zero. The contributions of the CI lowering for both calculations are also the same. This result may mean that the dissociated case does not form a bound state as we previously expected. The mechanism of the adsorption of nitrogen above the first layer of a Ti surface could be more complicated than we thought.

Table V-9 Comparisons of total energies, CI lowerings, and binding energies between Calculation I and Calculation II for the dissociated case. Where, Calculation I used 66 basis functions while Calculation II employed 74 basis functions for the entire $Ti_{26}N_2$ system.

Case	Total energy (in a.u.)	CI lowering (in a.u.)	Binding energy (in a.u.)
Calculation I	-116.491	0.096	-0.283
Calculation II	-116.513	0.095	-0.261

CHAPTER VI

DISCUSSION

VI-1 The Xα-SW Method Results for the Electronic Structure of Ti_x and Ti_xH Clusters.

In Chapter III, we described the calculated results of the electronic structure studies of Ti_4, Ti_7, and Ti_{13} clusters. These results showed that the electronic configuration for the titanium atom in bulk Ti metal is likely to be $(3\underline{d})^3$ $(4\underline{s})^1$. Therefore this configuration was chosen for the SCF-CI calculations on the chemisorption of nitrogen on Ti(0001).

After carrying out our new SCF-Xα-SW calculations, we have a better understanding of the role of the $\underline{d}$ electron in transition metal bonding. Method dependence has been recognized as the major reason for different conclusions.[30] This probably is true because different methods have various assumptions. Our calculated results show that the well surrounded Ti atoms have no $\underline{d}$ electron participation in the most active σ bonding orbitals while the others (refer to surface atoms) have certain amounts of $\underline{d}$ electrons participation in the most active σ bonding. Thus, a method dealing with the bulk Ti atom is predicted to have no $\underline{d}$ electron participation in the Ti - Ti bonding, and a method describing the surface Ti atom is expected to possess some $\underline{d}$ electron participation in the Ti - Ti bonding.

Salahub and Messmer,[85] in their studies of magnetic properties of V_{15}, Cr_{15}, and Fe_{15} clusters, concluded that the unrestricted Xα-SW method is capable of verifying the magnetic properties of transition metals. Our calculated results of Ti_4, Ti_7, and Ti_{13} clusters show that these titanium clusters still have high net magneton numbers which are expected to vanish in the limit of large cluster size of Ti metal. This may be due to two reasons; (a) our cluster size is too small to include the effect of the second neighbors, (b) Salahub and Messmer identified the ground state by occupying the lower orbitals up to the Fermi energy, while we verified a ground state by looking at the lowest total energy.

The studies of the hydrogen atom on Ti_4 and Ti_{13} clusters show a significant enhancement of d electron participation in Ti-Ti σ bonding. Due to the small amount of electronic charge participation of the hydrogen atom on the Ti_4 cluster, we are not able to see a large charge transfer among Ti atoms. However, our results hint that the presence of an H atom changes the nature of the Ti-Ti bonding from pure metallic to mixed metallic-ionic. The hydrogen compound studies of HTi_4 and HNi_4 indicate that the Ti_4-H bond is stronger than the Ni_4-H bond and hence we understand why only the Ti film exhibits H contamination while the Ni film does not.[67]

Our Xα-SW calculation of HTi_4 and Ti_4H clusters showed the capability of determining the geometry of the hydrogen atom on the Ti surface. However, this has to be done with caution. In Section

V-5 we discussed the danger of only using this single piece of evidence. Because of the muffin-tin approximation, our Xα-SW method is not able to provide an accurate total energy. Therefore, this method is not capable of determining the geometry of the chemisorption system precisely. Geometry may be determined by replacing the numerical basis set by an analytic basis set. The SCF-Xα-SW method without the muffin-tin approximation can have an accurate total energy.[87-89] However, we have to pay the price of a large consumption of computer time.

VI-2 SCF-CI Method on the Chemisorption Studies of Nitrogen on Ti(0001)

In Chapter V, we used the SCF-CI method to carry out the Ti_{10}-N_2 small cluster calculations and the Ti_{26}-N_2 larger cluster calculations. The results of the small cluster calculations gave important preliminary information about the potential surface for N_2 on Ti(0001). This information enabled us to select the most important geometries in performing SCF-CI calculations in the large cluster model. Our calculated results of the large cluster model show that the underlayer octahedral case is strongly bound and the overlayer perpendicular case is almost bound. The underlayer octahedral case has a large binding energy of 115 kcal/mole which is larger than the Fromm and Mayer's[79] experimental value, 80 kcal/mole. This implies that the lattice model we use may not readily yield an accurate underlayer calculation. In performing the underlayer calculation, we neglected the second neighbor effect on the second layer. The overlayer calculations, however, are more reliable since we included more surface atoms in our calculations. The overlayer perpendicular case might be bound if the molecule was stretched by 0.5 a.u. or so. This conclusion is from results obtained for CO on Ti.[86] Furthermore, other overlayer formation cases could turn out to be bound by considering stretched geometries.

Configuration interaction theory, in principle, permits an accurate determination of, (a) molecular potential curves, (b) equilibrium geometries, (c) the energetics of bonding, and (d) electronic spectra. However, our conclusions were mainly obtained from the SCF

calculation while the CI calculations do not have major effects. This hints that our method of calculations may still need improvement.

In spite of the minor deficiencies of the SCF-CI method, our results indicate the underlayer formation of N_2 on Ti(0001). This is in agreement with the LEED experimental result.

VI-3 Concluding Remarks

We applied the SCF-Xα-SW and SCF-CI methods to conduct the chemisorption studies of hydrogen and nitrogen on Ti(0001). Through these studies, we learned that these two methods possess different characteristics. The SCF-Xα-SW method has a property of rapid convergency and provides a good description of the energy spectrum of a given system. The SCF-Xα-SW method is also able to decompose the orbitals and extract the detailed information of electronic structure of the calculated system. The defects of the SCF-Xα-SW method are two fold: (1) The SCF-Xα-SW method we used employed the muffin-tin approximation, which leads to an inaccurate total energy. Thus the total energy is practically useless in determining the geometry of a chemisorbed system, (2) The SCF-Xα-SW method used the step searching process in computing, which encounters great difficulty in finding orbitals in a very dense spectrum. This confines the SCF-Xα-SW method to the small cluster calculations (for instance, titanium cluster size should be smaller than 30 atoms). The SCF-CI method, on the other hand, gives an accurate description of the total energy. Thus, this method can determine the geometry of a chemisorbed system by finding the lowest total energy among the possible geometries. The SCF-CI method also has two disadvantages. The first disadvantage is that the method does not give a good description of the energy spectrum near the Fermi energy region. This is because the highest occupied levels contain large contributions from cluster boundary atoms which in the present SCF-CI method are not well

described. The second disadvantage is that this method consumes a lot of computer time and becomes an expensive method due to the N^4 dependence of integrals required for a value of N contracted basis functions.

Despite the existence of problems of the SCF-Xα-SW and SCF-CI methods, both methods are important. It could be especially useful to apply both methods in studying one chemisorbed system. We believe that the complementarity of the two methods can give a much better understanding of the chemisorbed system. Of course, these methods also can be used independently in chemisorption studies.

BIBLIOGRAPHY

1. G. A. Somorjai, Principle of Surface Chemistry. p.228, Prentice-Hall, Inc., N. J. (1972).

2. E. W. Plummer, J. W. Gadzuk, and D. R. Penn, Physics Today 28, 63 (1973).

3. G. A. Somorjai, Accts. Chem. Res. 9, 248 (1976); Adv. Catalysis 26, 2 (1977).

4. G. C. Bond, Catalysis by Metal, (Academic, London, 1962).

5. See, for example: J. B. Pendry, Low Energy Electron Diffraction, (Academic, 1974).

6. J. E. Lennard - Jones, Trans. Faraday Soc. 28, 29 (1932).

7. J. R. Smith, S. C. Ying, and W. Kohn, Phys. Rev. Lett. 30, 610 (1973).

8. S. G. Davison and J. Koutecky, Proc. Phys. Soc. 89, 237 (1966).

9. D. Kalkstein and P. Soven, Surf. Sci. 26, 85 (1971).

10. G. P. Alldredge and L. Kleinman, Phys. Rev. B 10, 559 (1974).

11. For example: J. R. Schrieffer and R. Gomer, Surf. Sci. 25, 315 (1971); S. G. Davison and Y. S. Huang, Solid State Comm. 15, 863 (1974); E. A. Hyman, Phys. Rev. B 11, 3739 (1975).

12. J. C. Slater, Quantum Theory of Molecules and Solid (McGraw-Hill, New York, 1974); R. P. Messmer et al., Phys. Rev. B 13, 1396 (1976).

13. P. Hohenberg and W. Kohn, Phys. Rev. 135, B 864 (1964); W. Kohn and L. J. Sham, Phys. Rev. 140, A 1133 (1965).

14. K. H. Johnson and R. P. Messmer, J. Vac. Sci. Tech. 11, 236 (1974); N. Rosch and T. N. Rhodin, Phys. Rev. Lett. 32, 189 (1974).

15. J. L. Whitten and T. A. Pakkanen, Phys. Rev. B 21, 4357 (1980).

16. J. C. Slater, J. Chem. Phys. 43, S 228 (1965).

17. J. Korringa, Physica 13, 392 (1947).

18. W. Kohn and N. Rostoker, Phys. Rev. 94, 1111 (1954).

19. J. C. Slater, in Advances in Quantum Chemistry, edited by P. O. Lowdin (Academic, New York, 1972), Vol. 6, p. 1.

20. J. C. Slater, Quantum Theory of Molecules and Solids (McGraw-Hill, New York, 1974), Vol. 4.

21. J. W. D. Connolly and K. H. Johnson, Chem. Phys. Lett. 10, 616 (1971).

22. K. H. Johnson, J. G. Norman, Jr., and J. W. D. Connolly, in Computational Methods for Large Molecules and Localized States in Solids, edited by F. Herman, A. D. Mclean, and R. K. Nesbet (Plenum, New York, 1973), p. 161.

23. R. P. Messmer, S. K. Knudson, K. H. Johnson, J. B. Diamond and C. Y. Yang, Phys. Rev. B 13, 1396 (1976).

24. T. A. Pakkenen and J. L. Whitten, J. Chem. Phys. 69, 2168 (1978).

25. C. C. J. Roothaan, Rev. Mod. Phys. 23, 69 (1951).

26. C. C. J. Roothaan, Rev. Mod. Phys. 32, 179 (1960).

27. C. Edmiston and K. Ruedenberg, Rev. Mod. Phys. 35, 457 (1963)

28. H. Stoll and H. Preuss, Theoret. Chem. Acta (Berlin) 46, 11 (1977).

29. D. L. Wilhite and J. L. Whitten, J. Chem. Phys. 58, 948 (1973).

30. C. R. Fischer and J. L. Whitten, Phys. Rev. B 20, 1353 (1979).

31. C. F. Melius, J. W. Moskowitz, A. P. Mortola, M. B. Baille, and M. A. Ratner, Surf. Sci. 59, 279 (1976).

32. J. L. Whitten and M. Hackmayer, J. Chem. Phys. 51, 5584 (1969).

33. J. L. Whitten, J. Chem. Phys. 56, 5458 (1972).

34. L. deBroglie, Phil. Mag. 47, 446 (1924).

35. C. J. Davisson and L. Germer, Phys. Rev. 30, 705 (1927).

36. M. Laźnicka, LEED Surface Structure of Solid, International Summer School, Sponsored by the International Union of Crystallography, Printed by ÚKDŽ, (Smolenice Castle, Czechoslovakia, 1971).

37. H. D. Shih, F. Jona, D. W. Jepsen, and P. M. Marcus, J. Vac. Sci. Tech. 15, 596 (1976).

38. H. D. Shih, F. Jona, D. W. Jepsen, and P. M. Marcus, Phys. Rev. Lett. 36, 798 (1976).

39. G. A. Somorjai, Principle of Surface Chemistry (Prentice-Hall, 1972), p. 27.

40. C. Kittel, Introduction to Solid State Physics, 5th. edition, (John Wiley & Son, N. Y., 1978).

41. T. B. Grimley, J. Vac. Sci. Tech. 8, 31 (1971).

42. G. Ertl and J. Küppers, Surface Sci. 21, 61 (1970).

43. K. Siegbahn et al., ESCA - Atomic, Molecular and Solid State Structure Studied by Means of Electron Spectroscopy, Almquist and Wiksells Uppsala (1967).

44. D. E. Eastman, "Ultraviolet Photoelectron Spectroscopy Studies of Noble and Transition Metals" in "Electron Spectroscopy", edited by D. A. Shirley, (North-Halland Publishing Company, 1972), p. 487.

45. D. E. Eastman, J. Appl. Phys. 40, 1387 (1969).

46. H. Reather, J. Phys. Radium, 31, C1-59 (1970).

47. C. F. Melius, Chem. Phys. Lett. 39, 287 (1976).

48. A. B. Kunz, M. P. Guse, and R. J. Blint, J. Phys. 38, L358 (1975); R. J. Blint, A. B. Kunz, and M. P. Guse, Chem. Phys. Lett. 36, 191 (1975).

49. P. R. Scott and W. G. Richards, J. Phys. B 7, L347 (1974); P. R. Scott and W. G. Richards, J. Phys. B 7, 500 (1974).

50. T. A. Pakkanen, Ph.D. Thesis (State University of New York at Stony Brook, 1977) (unpublished).

51. D. A. Dowden, in Chemisorption, edited by W. E. Garner (Butterworth, London, 1958); H. Deuss and A. Van der Avoird, Phys. Rev. B 8, 2441 (1973).

52. R. P. Messmer, D. R. Salahub, K. H. Johnson, and C. Y. Yang, Chem, Phys. Lett. 51, 84 (1977).

53. N. Rosch and T. N. Rhodin, Phys. Rev. Lett. 32, 1189 (1974).

54. L. F. Matheiss, Phys. Rev. 134, A970 (1974).

55. W. Mueller, J. P. Blackledge, and G. G. Libowitz, Metal Hydrides, (Academic Press, New York, 1968).

56. S. J. Niemczyk and C. F. Melius, Chem. Phys. Lett. 46, 236 (1977).

57. R. P. Messmer, Surf. Sci. 106, 225 (1981).

58. I. H. Kahn, Surf. Sci. 52, 489 (1975).

59. G. Skinner, Titanium and its Compounds, (Herrick L. Johnston Enterprise, 1954), p. 3.

60. K. Schwarz, Phys. Rev. B 5, 2466 (1971).

61. R. B. Leighton, Principles of Modern Physics, (McGraw-Hill, New York, 1959), p. 249.

62. P. J. Feibelman, J. A. Appelbaum, and D. R. Hamann, Phys. Rev. B 20, 1433 (1979).

63. J. R. Anderson and N. Thompson, Surf. Sci. 26, 397 (1971), obtained -3.95 eV. Similar values have been obtained by many others, as reviewed by R. J. D'Arcy and N. A. Surplice, Surf. Sci. 36, 783 (1973). However, these latter authors believe that a higher value $\approx$4.2 - 5.6 eV is more characteristic of clean Ti.

64. D. P. Gregory, Sci. Am. 228, 13 (1973).

65. M. A. Pick, J. W. Davenport, M. Strongin, and G. J. Dienes, Phys. Rev. Lett. 43, 286 (1979).

66. P. J. Feibelman and D. R. Hamann, Phys. Rev. B 21, 1385 (1980).

67. P. J. Feibelman, D. R. Hamann, and F. J. Himpsel, Phys. Rev. B 22, 1734 (1980).

68. F. Jona, J. Phys. C 11, 4271 (1978).

69. J. R. Smith, F. J. Arlinghaus, and J. G. Gay, Solid Commun. 24, 279 (1977).

70. A. Liebsch, Phys. Rev. B 17, 1653 (1978).

71. C. S. Wang and A. J. Freeman, Phys. Rev. B 19, 4930 (1979).

72. D. E. Eastman, Solid State Commun. 10, 933 (1972).

73. P. Cremaschi and J. L. Whitten, Phys. Rev. Lett. 46, 1242 (1981).

74. J. R. Anderson, The Structure of Metallic Catalysis, (Academic Press, New York, 1975).

75. L. H. Bennett, ed., Electronic Density of States, National Bureau of Standards Special Publiscation 323, Washington, D. C. (1971).

76. D. E. Eastman, J. K. Cashion, and A. C. Switendick, Phys. Rev. Lett. 27, 35 (1971).

77. F. P. Mertons and R. P. Eischens, "The Structure and Chemistry of Solid Surfaces" edited by G. A. Somorjai, (John Wiley & Sons, 1968) p. 53-1.

78. D. A. King and F. C. Tompkins, Trans. Far. Soc. 64, 496 (1968).

79. E. Fromm and O. Mayer, Surf. Sci. 57, 775 (1976).

80. P. J. Feibelman and F. J. Himpsel, Phys. Rev. B 21, 1394 (1980).

81. H. D. Shih, F. Jona, D. W. Jepsen, and P. M. Marcus, Surf. Sci. 60, 445 (1976).

82. C. R. Fischer, S. C. Hung, and J. L. Whitten, Bull. Am. Phys. Soc. 27, 345 (1982).

83. J. L. Whitten, J.Chem. Phys. 44, 359 (1966).

84. H. F. Schaefer, The Electronic Structure of Atoms and Molecules, (Addison - Wesley, 1972) p. 148 to p. 152.

85. D. R. Salahub and R. P. Messmer, Surf. Sci. 106, 415 (1981).

86. C. R. Fischer, L. A. Burke and J. L. Whitten, Phys. Rev. Lett. 49, 344 (1982).

87. E.J. Baerends, D.E. Ellis, and P. Ros, Chem. Phys. 2, 41 (1973).

88. E.J. Baerends and P. Ros, Chem. Phys. 8, 412 (1975).

89. E.J. Baerends and P. Ros, Int. J. Quantum Chem. S12, 169 (1978).